universität wien

# MASTERARBEIT / MASTER'S THESIS

Titel der Masterarbeit / Title of the Master's Thesis

„Towards an understanding of membrane binding properties of MRCK"

verfasst von / submitted by

Elisabeth Fuchs, BSc

angestrebter akademischer Grad / in partial fulfilment of the requirements for the degree of

Master of Science (MSc)

Wien, 2016 / Vienna 2016

| | |
|---|---|
| Studienkennzahl lt. Studienblatt / degree programme code as it appears on the student record sheet: | A 066 834 |
| Studienrichtung lt. Studienblatt / degree programme as it appears on the student record sheet: | Masterstudium Molekulare Biologie |
| Betreut von / Supervisor: | Thomas A. Leonard, Assoc. Prof. PhD. |
| Mitbetreut von / Co-Supervisor: | |

# TABLE OF CONTENTS

# 1 INTRODUCTION

## 1.1 The small GTPase Cdc42 is important for the regulation of the actin cytoskeleton

Cdc42 is a small GTPase that, together with RhoA and Rac1, belongs to the Rho family of GTPases that in turn is part of the Ras superfamily. Small GTPases like Cdc42 and Rac1 function as molecular switches in a variety of signaling pathways that lead to actin reorganization, and therefore cell proliferation, migration and cell polarity, cell cycle progression, and endocytosis (Stengel & Zheng 2011; Chircop 2014; Melendez et al. 2011; Pollard & Cooper 2009). Cdc42, like other small GTPases, switches between an inactive GDP-bound and an active GTP-bound state in response to a variety of extracellular stimuli, e.g. cytokines, mitogens, or growth factors, but also intracellular factors can lead to activation of the Rho GTPase. In the active state, Cdc42 translocates from the cytosol to the membrane, binds to one of its effector proteins, and thereby activating a variety of different signaling cascades. Whether Cdc42 is active or inactive is regulated through the interaction with guanine nucleotide exchange factors (GEFs), GTPase activating proteins (GAPs), and guanosine nucleotide dissociation inhibitors (GDIs). GEFs activate the GTPase by stimulating the release of GDP and thereby allowing binding of GTP. GAPs bind to the active GTPases and promote hydrolysis of GTP to GDP leading to inactivation of the GTPase. Attached at its carboxyl terminus, Cdc42 has a geranylgeranyl lipid anchor important for interaction with the membrane. Besides Cdc42's activation state, its localization to the membrane is important to be tightly regulated to ensure proper signaling. GDIs bind to inactive GTPases to prevent localization to the membrane and activation. Once Cdc42 is in the activated state, it acts via its many effector proteins to activate different signaling cascades.

Interaction of Cdc42 with its effector proteins is mediated by the so called effector or switch I domain of Cdc42, comprising residues 26 to 50 (Johnson 1999). The binding of effector proteins like p21 activated kinase PAK, activated Cdc42 kinase ACK, and Wiskott–Aldrich Syndrome protein WASP involves also interaction with the switch II region (residues 57–74) but the switch I region is the predominant interacting surface (Chandrashekar et al. 2011). The effector domain is highly

conserved among Cdc42 proteins, and forms an extended loop structure enabling effector binding (Johnson 1999). One of Cdc42's many effector proteins is MRCK (myotonic dystrophy kinase related Cdc42 binding kinase) (Johnson 1999; Chircop 2014; Melendez et al. 2011).

## 1.2 Myotonic dystrophy kinase related Cdc42 binding kinase

MRCK is a member of the AGC superfamily of serine/threonine protein kinases and belongs together with Rho-associated coiled-coil kinase (ROCK), Citron Rho-interacting kinase (CRIK), and dystrophia myotonica protein kinase (DMPK) to the DMPK protein family. There are three different isoforms of MRCK in mammals: MRCKα, MRCKβ, and MRCKγ. MRCKγ was first identified in 2004 when searching for proteins with a Cdc42/Rac1 interactive binding (CRIB) domain (Ng et al. 2004). It differs from the other MRCK isoforms in having a much shorter coiled coil region and is thus, at 170 kDa, smaller than MRCKα and β (approximately 195 kDa). MRCKα and β share 85% sequence identity and are thus closely related (Ng et al. 2004).

## 1.3 Domain organization of MRCK

The amino terminal kinase domain is followed by a coiled coil region that separates the catalytic region from the regulatory region and is important for dimerization of two MRCK proteins (Ivan Tan et al. 2001). The coiled coil domain is followed by a protein kinase C conserved region 1 (C1) domain, a pleckstrin homology (PH) domain, and a citron homology (CNH) domain (Unbekandt & Olson 2014) (Figure 1). The C1 domain is a zinc finger structure that was first characterized in PKC to recognize diacylglycerol, a second messenger signaling lipid (Ono et al. 1989). Phorbol esters are used to mimic diacylglycerol, which is known to activate PKC at the membrane through interaction with the C1 domain (Wu-Zhang & Newton 2013).The C1 domain of MRCK was shown to bind to phorbol esters as well but with lower binding affinities than the PKCα and PKCδ C1b domains. Moreover, MRCK C1 domain's binding affinity for DAG lactones are 1000 fold lower than for phorbol esters. This huge difference in binding affinities for phorbol esters and DAG lactones could not be observed for PKCα and δ (Sung et al. 2008). This fact leads to the question, whether the C1 domain of MRCK is responsible for binding to DAG or whether other regions of MRCK are contributing to this interaction. It is speculated that the interaction of the

C1 domain with DAG plays a role in the translocation of MRCK to the membrane, since addition of phorbol 12-myristate 13-acetate (PMA), a diacylglycerol mimic, leads to translocation of MRCK from the cytoplasm to the membrane (Leung et al. 1998; Sung et al. 2008; Ivan Tan et al. 2001).

The Pleckstrin Homology (PH) domain may be another contributor in membrane targeting of MRCK, since many PH domains target their host protein to the membrane by binding to phosphoinositides (Lemmon & Ferguson 2000; Unbekandt & Olson 2014) but no studies to date have explicitly addressed the role of the PH domain of MRCK.

Adjacent to the PH domain is the Citron Homology (CNH) domain, a domain of unknown structure and function, which was identified in the related Citron Rho-interacting kinase CRIK. The CNH domain is also found in other kinases like the TRAF2 and NCK-interacting protein kinase (TNIK) and Misshapen-like kinase 1 (MINK) (Hussain et al. 2010; Mikryukov & Moss 2012), but also in the lysosomal tethering factor Vam6p and in the yeast Rho1-GEF Rom1 (Caplan et al. 2001). In the Vam6p protein the CNH domain is important for the interaction with lysosomes through interaction with lipids or proteins at the lysosomal membrane (Caplan et al. 2001). The CNH domain of TNIK and Mitogen-activated protein kinase kinase kinase kinase (MAP4K) has been shown to mediate the interaction with the small GTPase Rap2 (Hussain et al. 2010) and in TNIK but also in MINK the CNH domain interacts with the kinase domain leading to kinase inactivation (Mikryukov & Moss 2012). Nevertheless, the role of the CNH domain of MRCK has not been explicitly addressed in any study to date.

At the very C-terminus of the protein is the Cdc42/Rac1 interactive binding (CRIB) domain which binds to Cdc42 and with weaker affinity to Rac1 (Unbekandt & Olson 2014; Leung et al. 1998). As its name implies, MRCK was first identified based on its interaction with Cdc42. This interaction does not lead to MRCK activation but it is rather important for localization to the membrane (Leung et al. 1998; Ivan Tan et al. 2001).

## 1.4 The Cdc42-binding CRIB domain

In 1995 Burbelo et al. defined the minimal CRIB domain with eight core amino acids being ISXP$(X)_{2-4}$FXHXXHVG. They showed that this Cdc42/Rac interactive binding

domain only binds to the GTP loaded form of Cdc42 and that proteins, which vary in one or two amino acids of the core sequence are still able to bind to Cdc42 (Burbelo et al. 1995). Later, it was investigated that this consensus CRIB sequence is essential for the binding to effector proteins but that further sequences are required for high affinity binding. It was also suggested that the CRIB domain is in an unfolded state in the absence of Cdc42 binding (Stevens et al. 1999) and in the case of some CRIB-containing kinases, binding of Cdc42 led to structuring of the CRIB peptide (Stevens et al. 1999; Mott et al. 1999). Binding of Cdc42 to CRIB domains of different kinases like the non-receptor tyrosine kinase ACK, p21-activated kinase PAK, and Wiskott-Aldrich syndrome protein (WASP) was investigated in more detail revealing binding affinities in the nanomolar range (Mott et al. 1999; Garrard et al. 2003; Rudolph et al. 1998).

## 1.5 Regulation of MRCK's kinase activity

MRCK forms multimeric complexes through parallel intermolecular interactions of the coiled coil domains mediated through dimerization of the kinase domains. The dimerization together with intermolecular trans-autophosphorylation of residues located in the activation loop of the kinase domain has been suggested to be important for kinase activity (Ivan Tan et al. 2001). Moreover, a part of the coiled coil region (the so called kinase inhibitory motif KIM (Ng et al. 2004; Ivan Tan et al. 2001)) can interact with the kinase domain and negatively regulate kinase activity. Hence, the amino-terminal dimerization together with the coiled coil mediated inhibition determines the catalytic state of MRCK. It is hypothesized, that binding of MRCK to PMA increases the kinase activity, possibly by disrupting the interaction of the coiled coil region with the kinase domain (Ivan Tan et al. 2001). Heikkila et al. were able to solve the crystal structure of the kinase domain of MRCKβ, verifying the dimeric state of the kinase domain. The crystal structure showed that the dimerization of the kinase domains is facilitated through binding of the C-terminus of the kinase domain to the four N-terminal helices and that this dimeric state reflects the active kinase conformation. The active, dimeric state was found to occur in the absence of activation loop phosphorylation (Heikkila et al. 2011).

## 1.6 MRCK and its substrates

Leung et al. identified some MRCKα substrates, e.g. myelin basic protein, histone H1, and non-muscle myosin regulatory light chain (MLC2) (Leung et al. 1998). MRCK phosphorylates its substrates on serine and/or threonine residues with MLC2 being one of its most prominent substrates. Non-muscle myosin 2 (NM2) belongs to the myosin superfamily of actin-based molecular motors that can reversibly bind to actin filaments, and hydrolyze ATP to generate mechanical force. Thus, NM2 is essential for processes in the cell that require cell migration, cellular reshaping, cell adhesion, or cell division, and it is important for actin crosslinking and contractile functions of the cell (Conti & Adelstein 2008; Vicente-Manzanares et al. 2009). NM2 is a hexamer comprising three different proteins: two heavy chains, two essential light chains (ELCs), and two regulatory light chains ((R)MLCs). Regulation of non-muscle myosin 2 is mediated by phosphorylation of the regulatory light chains on serine 19 and/or threonine 18 by different kinases, e.g. ROCK or MRCK. Phosphorylation of serine 19 leads to activation of NM2 (Vicente-Manzanares et al. 2009). Protein Phosphatase 1 (PP1) dephosphorylates and thereby inactivates non-muscle myosin 2. Therefore, an indirect way of activating NM2 is phosphorylation and inactivation of PP1 via phosphorylation of myosin phosphatase target subunit 1 (MYPT1) (Vicente-Manzanares et al. 2009). MRCK together with ROCK and myosin light chain kinase (MLCK) regulates the phosphorylation of myosin light chain (MLC2) either directly through serine 19 phosphorylation or indirectly via phosphorylation of myosin phosphatase targeting subunit 1 (MYPT1) of protein phosphatase 1. In this way, MRCK contributes to the actin-myosin contractility important for cell movement and invasion (Wilkinson et al. 2005). Similarly, the *C. elegans* isoform of MRCK was found to be responsible for myosin activation and therefore actin-myosin contraction (Gally et al. 2009), while the *D. melanogaster* MRCK homolog Genghis Khan (GEK) has been shown to be important for the distribution of F-actin and actin-binding proteins in germ line cells (Luo et al. 1997).

## 1.7 Cellular functions of MRCK

Many studies have investigated the role of MRCK in the regulation of the actin cytoskeleton. MRCK has been shown to phosphorylate moesin leading to filopodia

formation important for migration (Nakamura et al. 2000). In line with MRCK's role in the regulation of the actin cytoskeleton, it is important for the reorientation of the microtubule-organizing center in migrating cells and for the rearward nuclear movement regulated through phosphorylation of non-muscle myosin 2 (Gomes et al. 2005). A tripartite complex of MRCK, adaptor protein LRAP35, and myosin II-like myosin heavy chain (MYO18A) co-localizes with lamellar actomyosin filaments, promoting phosphorylation of the regulatory myosin light chain (MLC) by MRCK, and thereby regulating the retrograde flow in the lamella leading to membrane protrusion and cell migration (Tan et al. 2008). Complex formation of MRCK with another adaptor protein (LRAP25) and LIM kinase 1 was shown to regulate F-actin dynamics via regulation of cofilin activity through the LIM kinase. Thus, MRCK is not only localized in lamella but also in the lamellipodia of motile cells (Lee et al. 2014). The tight junction protein ZO-1 interacts with MRCKβ and targets it to the leading edge of migrating cells. This interaction is dependent on Cdc42 binding and necessary for polarized cell migration (Huo et al. 2011). In addition, PDK1 interacts with and activates MRCKα at the membrane leading to lamellipodia retraction and thus epithelial directional migration and invasion (Gagliardi et al. 2014). To summarize, MRCK is important for actin-myosin regulation which is connected to cell motility via interaction with different proteins and signaling cascades. It is not surprising, therefore, that MRCK has been implicated in different types of cancer, e.g. cutaneous squamous cell carcinoma, breast cancer, or prostate cancer (Heikkila et al. 2011; Unbekandt et al. 2014; Lowe et al. 2012).

## 1.8 Open questions

Very few studies to date have addressed the C-terminal regulatory region of MRCK and there is no crystal structure available. Therefore, the role of these domains in localizing MRCK to membranes, their putative lipid ligands, and their arrangement in the three dimensional structure are still uncharacterized. It has been speculated that the C1 domain is binding with low affinity to diacylglycerol, and that the PH domain may be involved in membrane binding, but the function of the CNH domain in MRCK is completely unknown. To better understand MRCK's interaction with and localization to cellular membranes it is important to understand how these regulatory domains function as single domains but also how they might interact to function as

one construct in mediating membrane localization of MRCK. The fourth regulatory region of MRCK at the very C-terminus is the Cdc42/Rac1 interactive binding CRIB domain. This domain has been shown to bind to Cdc42 and to Rac1 and thereby trigger membrane translocation of MRCK. Although the interaction of Cdc42 with CRIB domains of Cdc42 binding proteins e.g. PAK, ACK, and WASP has been investigated on a biochemical and structural basis revealing binding affinities in the nanomolar range, MRCK's interaction with Cdc42 has been validated by co-immunoprecipitation and western blotting but has not been quantified in vitro.

## 1.9 Aim of this thesis

The interaction of MRCK with cellular membranes and Cdc42 is important for MRCK's localization to the membrane and for the regulation of kinase activity, and, moreover, interaction with Cdc42 was crucial for identification of MRCK. While the interaction between Cdc42 and MRCK was identified in a screen for effector proteins by co-IP and Western blotting, the interaction has not been confirmed or quantitated in vitro. Furthermore, no attempts were made to understand the role of MRCK's regulatory domains. Therefore, this master's thesis addresses two aims:

1) What is the structure of the C-terminal domains of MRCK, in particular its CNH domain, and how do the C-terminal domains target MRCK to membranes in the cell?
2) What is the binding affinity between MRCK and Cdc42, and how does this interaction influence MRCK targeting to membranes?

# 2 MATERIALS AND METHODS

## 2.1 Cloning of protein constructs

### *2.1.1 Cloning and expression of CeMRCK1 955-1517 in Sf9 insect cells*

50 µl PCR reaction was set up according to manufacturer's protocol using Phusion Hot Start DNA polymerase (Thermo Fisher Scientific). A plasmid containing the CeMRCK1 955-1592 was used as template, as forward primer 5'-TGACTACGCGCGCGAACGAGGTCATAACTTTGAGAGAATG-3' and as reverse primer 5'-ATAGGTGCGGCCGCTTATTTCCGTCCATCAGTGCTTCCAG-3' were used. PCR reaction was followed by PCR purification using the QIAquick PCR purification kit from QIAGEN. Digestion with restriction enzymes (BssHII for 3 hours at 50°C, NotI for minimum 3 hours or overnight at 37°C) was performed using CutSmart Buffer (New England Biosience). Restriction enzymes were deactivated either by heat inactivation at 65°C or by PCR purification. For ligation of the insert into the pFastBac Dual vector with T4 DNA ligase an insert to vector ratio of 1:3 was used. After incubation for 3 hours at room temperature, 5 µl of the ligation reaction were added to 20 µl of DH10β electro-competent *E. coli* cells diluted with 80 µl of cold $dH_2O$. After 1 hour incubation at 37°C shaking at 170 rpm cells were plated on LB agar plates containing 100 µg/ml ampicillin. Colony PCR to confirm successful ligation was performed using 2x DreamTaq Green PCR Master Mix (Thermo Fisher scientific). Liquid cultures (LB containing 100 µg/ml ampicillin) of picked colonies were grown overnight at 37°C, 170 rpm. Centrifugation for 10 minutes at 4500 rpm was followed by plasmid isolation using the QIAquick Spin Miniprep kit, according to manufacturer's protocol (QIAGEN). Positive colonies were confirmed by DNA sequencing of the insert.

For generation of recombinant bacmid the pFastBac construct was transformed into chemically competent DH10EmBacY *E. coli*. Cells were incubated with ~100 ng of DNA for 30 minutes on ice, followed by heat shock at 42°C for 40 seconds. 750 µl of LB were added, followed by incubation for 5 to 6 hours at 37°C, 170 rpm. Cells were plated on LB agar plates containing 50 µg/ml kanamycin, 7 µg/ml gentamicin, 10 µg/ml tetracycline, 200 µg/ml X-gal, and 40 µg/ml Isopropyl β-D-thiogalactoside. Plates were incubated for 48 hours at 37°C. White colonies were

tested for positive transposition by colony PCR using M13 forward and reverse primers (2x Dream taq green master mix) and liquid cultures were grown (LB containing 50 µg/ml kanamycin, 7 µg/ml gentamicin, and 10 µg/ml tetracycline) at 37°C, 170 rpm for ~8 hours. Liquid cultures were centrifuged for 10 minutes at 4000 rpm followed by isolation of the recombinant bacmid DNA. The cell pellet was resuspended in 300 µl of resuspension buffer P1 (Qiagen). 300 µl of lysis buffer P2 (Qiagen) was added and the sample was incubated for 4 minutes at room temperature. 300 µl neutralization buffer N3 (Qiagen) was added, mixed and incubated for 10 minutes on ice. The sample was centrifuged at RT at 13000 x g for 10 minutes. The supernatant was added to 800 µl isopropanol, followed by incubation on ice for 10 minutes and centrifugation for 15 minutes. The pellet was washed with 500 µl 70% ethanol and centrifuged for 5 minutes. The supernatant was aspirated and the pellet was air dried for a minimum of 10 minutes. 40 µl of $dH_2O$ were added to the dried pellet followed by incubation at 70°C for 10 minutes to resuspend the DNA and sterilize it prior to transfection.

For transfection of Sf9 cells, 2.5 µg of bacmid DNA were mixed with 100 µl of ESF medium, and 5 µl of Fugene transfection reagent (Promega) was mixed with 50 µl of ESF medium; both mixtures were incubated for 5 minutes before combining them. After incubation for 20 to 30 minutes at room temperature the sample was added to a well of a 6 well plate containing 3 ml of 1 x $10^6$ cells. Cells started to become fluorescent 3 to 6 days after transfection and the supernatant (V0) was harvested when most cells exhibited fluorescence (YFP expression). With this V0 a 25 ml culture of 1 x $10^6$ Sf9 insect cells/ml were infected and after three to five days after infection, at ~90% cell viability, a V1 viral stock was harvested. Briefly, the 25 ml culture was centrifuged at 500 x g for 10 minutes and the supernatant (V1) was collected and stored at 4°C. For expression of recombinant protein for purification, a 1 l culture of Sf9 insect cells (1 x $10^6$ cells) was infected with 1 ml of the V1 virus. Cells were grown for some days until viability dropped below 90%. Cells were spun down for 25 minutes at 3500 rpm, the supernatant was discarded and the cell pellets were frozen in liquid nitrogen and stored at -80°C.

### *2.1.2 Cloning of hsRac1 in* E.coli

50 µl PCR reaction was set up according to manufacturer's protocol using Phusion Hot Start DNA polymerase (Thermo Fisher Scientific) and HeLa cell cDNA as template. 5'-GTAGTCAGGATCCATGCAGGCCATCAAGTGTGTGGTGG-3' and 5'-GTAGTCAGCGGCCGCTTAGCAGAGGACTGCTCGGATCGC-3' were used as forward and reverse primers, respectively. Efficiency of PCR reaction was checked on a 1% agarose gel followed by PCR purification using the QIAquick PCR purification kit from QIAGEN. Digestion with restriction enzymes BamHI and NotI overnight at 37°C was accomplished using CutSmart Buffer (New England Biosience). Restriction enzymes were deactivated via QIAquick PCR purification according to manufacturer's protocol. For ligation of the insert into the pGSTII BamHI/NotI vector with T4 DNA ligase an insert to vector ratio of 1:3 was used. After incubation for 3 hours at room temperature 5 µl of ligate was added to 20 µl of DH10β electro-competent *E. coli* cells diluted with 80 µl of $dH_2O$. After 1 hour incubation at 37°C, cells were plated on LB agar plates containing 100 µg/ml ampicillin. To test whether ligation worked or not, colony PCR was performed using 2x DreamTaq Green PCR Master Mix (Thermo Fisher scientific). Liquid cultures (LB containing 100 µg/ml ampicillin) of picked colonies were shaking overnight at 37°C. Centrifugation for 10 minutes at 4500 rpm was followed by QIAquick Spin Miniprep according to manufacturer's protocol (QIAGEN) and DNA was sent for sequencing. Transformation into BL21* *E. coli* was accomplished via electroporation. LB was added to the cells after electroporation and the liquid culture was left shaking for approximately 30 minutes before plating on a LB agar plate containing 100 µg/ml ampicillin. From one single colony an overnight liquid culture was started and on the next day this liquid culture was diluted to an $OD_{600}$ of 0.05 in 1 l LB containing 100 µg/ml ampicillin. The liquid cell culture was left shaking at 37°C, 170 rpm until an $OD_{600}$ of ~0.8 was reached before induction of protein expression with 200 µM IPTG. Cells were left shaking at 22°C overnight before they were centrifuged for 20 minutes at 4000 rpm. The pellet was resuspended in buffer (50 mM Tris pH 7.5, 150 mM $MgCl_2$; 1 mM TCEP), frozen in liquid nitrogen and stored at -80°C.

### *2.1.3 Cloning and expression of the CRIB peptide in* E. coli

GST-tagged CRIB peptide 5'-QISTPSDFMHIVHMGPAPVMELQQNFIDLQ-3' was cloned by following the same cloning protocol used to clone HsRac1. 5'-GTAGTCAGGATCCCAAATCTCGACCCCATCGGATTTC-3' was used as a forward primer. 5'-TGACTACGCGGCCGCTTACTGCAAGTCAATGAAATTTTGTTGTAG-3' was used as the reverse primer. Efficiency of PCR was checked on a 2% agarose gel. BamHI and NotI were used as restriction enzymes. Protein was expressed in *E. coli*, harvested, and resuspended in buffer (50 mM Tris pH 7.4, 150 mM KCl, 2 mM $MgCl_2$, 1 mM TCEP), frozen in liquid nitrogen, and stored at -80°C.

### *2.1.4 Cloning and expression of MBP-Cdc42 in* E. coli

MBP-Cdc42 fusion protein was cloned using overlap extension PCR. For this, Cdc42 was cloned with a 5' overlap, and MBP was cloned with the complementary 3' overlap.

For MBP the T7 forward primer (5'-TAATACGACTCACTATAGGGG-3') and 5'-CAACAACACACTTAATTGTCTGCCCACTTCCAGTCTGCGCGTCTTTCAGG-3' as reverse primer were used. Cdc42 was cloned using 5' – CCTGAAAGACGCGCAGACTGGAAGTGGGCAGACAATTAAGTGTGTTGTTG-3' and 5'-CCGCTTACAGACAAGCTGTGACCGT-3' (pGST sequencing primer) as forward and reverse primers, respectively. For Cdc42 pGST2 II vector and for MBP the pHis II vector was used as templates. 50 µl PCR reaction was set up according to manufacturer's protocol using Phusion Hot Start DNA polymerase (Thermo Fisher Scientific).

For the overlap extension PCR, the products of the two initial PCR reactions were mixed stoichiometrically. PCR reaction was set up using 2x DreamTaq Green PCR Master Mix (Thermo Fisher scientific). After the first 6 cycles of PCR, MBP-forward (5'- TGACTACCCATGGGGAAAATCGAAGAAGGTAAACTGG-3') and Cdc42-reverse (5'-TGGTACCGCGGCCGCTTACTCGAGGGCAGCTAGGATAGC-3') primers were added. PCR was continued for 34 cycles. Further cloning of MBP-Cdc42 was done according to Rac1 cloning for expression in E. coli. pHisII vector was used as a template. NcoI and NotI were used as restriction enzymes. The cell pellet was resuspended in buffer (50 mM Tris pH 7.5, 150 mM KCl, 2mM $MgCl_2$, 1 mM TCEP), frozen in liquid nitrogen, and stored at -80°C.

### *2.1.5 Expression of selenomethionine labeled proteins in Sf9 insect cells*

A 25 ml suspension Sf9 cell stock was transferred from standard ESF medium (Expression Systems) to ESF methionine deficient medium (Expression Systems) when cell density reached 4 x $10^6$ cells/ml. This 25 ml methionine free suspension culture was grown for two days in order to start a 90 ml culture using methione-deficient ESF medium. After three days the cells were split to obtain a 1 l culture with 0.7 x $10^6$ cells/ml. 24 hours later insect cells were infected with 1 ml V1 of CeMRCK1 construct. Selenomethionine (5 mg in 100 ml methionine deficient ESF medium) was added in regular intervals to the culture, starting 8 hours after infection and then every 24 hours after infection until viability dropped below 90% (3 to 5 days after infection). Cells were harvested (3500 rpm, 25 minutes), the cell pellet was frozen in liquid nitrogen, and stored at -80°C.

## 2.2 Protein purification

### *2.2.1 Purification of CeMRCK1 955-1592, selenomethionine-substituted CeMRCK1 955-1592, and CeMRCK1 955-1517*

Sf9 cell pellets were resuspended in lysis buffer (50 mM HEPES pH 8.0, 150 mM KCl, 20 mM imidazole, 1 mM TCEP) with 2 mM $MgCl_2$, 2 mM benzamidine, 50 µl 100x protease inhibitor mix (P8849 Sigma), 1 µl benzonase, and 1 mM PMSF. The resuspended cells were incubated on ice for 30 minutes, and then centrifuged for 30 minutes at 18000 rpm, 4°C. The supernatant was loaded onto a washed and equilibrated 5 ml HisTrap FF column (GE Healthcare Life Sciences), followed by gradient elution with elution buffer (50 mM HEPES pH 8, 150 mM KCl, 1 M imidazole, 1 mM TCEP). Peak fractions were pooled and 1:1 diluted with lysis buffer. 150 µl of TEV (2 mg/ml) were added and the cleavage reaction was incubated at 4°C over night. The sample was further diluted 1:4 with $S_A$ buffer (50 mM Tris pH 8, 1 mM TCEP) to lower the salt concentration for binding to a cation exchange column. The sample was then loaded onto a 5 ml HiTrap SP FF column (GE Healthcare Life Sciences) followed by gradient elution with elution buffer $S_B$ (50 mM Tris pH 8, 1 M NaCl, 1 mM TCEP). Peak fractions were pooled, concentrated and loaded to a HiLoad 16/600 Superdex 75 column (GE Healthcare Life Sciences) equilibrated with gel filtration buffer (20 mM Tris pH 7.5, 150 mM KCl, 1 mM TCEP, 1% glycerol). Peak

fractions were pooled and concentrated to 4 mg/ml and the protein was frozen in liquid nitrogen and stored at -80°C. For the selenomethionine-substituted protein, the final gel filtration was replaced by four concentration/dilution steps to buffer exchange the protein.

### *2.2.2 Purification of HsCdc42 and HsRac1*

Cell pellets were resuspended in lysis buffer (50 mM Tris pH 7.4, 150 mM KCl, 2 mM $MgCl_2$, 1 mM TCEP, 2 mM benzamidine), and flash frozen in liquid nitrogen. Frozen pellets were thawed, and 0.2 mg/ml lysozyme and 2 µl benzonase were added. The reaction mix was incubated on ice for 30 minutes, followed by sonication (sonifier WD-450D) three times for one minute and centrifugation at 18000 rpm for 15 minutes. 1 ml of equilibrated Glutathione Sepharose 4B beads (GE Healthcare Life Science) was added to 50 ml supernatant and the lysate was incubated for 3 hours rotating at 4°C followed by centrifugation at 500 x g for 5 minutes. Beads were washed with buffer (50 mM Tris pH 7.4, 150 mM KCl, 2 mM $MgCl_2$, 1 mM TCEP), resuspended in 15 ml buffer, and cleaved with 150 µl of TEV (2 mg/ml) overnight rotating at 4°C. Beads were centrifuged and the supernatant containing the protein was collected, concentrated and loaded on a washed and equilibrated Superdex 75 16/600 gel filtration column. Peak fractions were pooled and concentrated, frozen in liquid nitrogen, and stored at -80°C.

### *2.2.3 Purification of MBP-Cdc42*

The cell pellet was thawed, 0.2 mg/ml lysozyme, 2 mM benzamidine, and 1 µl benzonase were added, and the sample was incubated on ice for 30 minutes, followed by two cycles of sonication (2 minutes at 50% power). The sonicated sample was centrifuged for 30 minutes at 18000 rpm, 4°C, and the supernatant was loaded to a 1 ml HisTrap column (equilibrated with 50 mM Tris pH 7.5, 150 mM KCl, 2 mM $MgCl_2$, 1 mM TCEP), followed by gradient elution with elution buffer (50 mM Tris pH 7.5, 150 mM KCl, 2 mM $MgCl_2$, 1 mM TCEP, 1 M imidazole). Peak fractions were pooled and incubated with TEV protease overnight. The TEV-cleaved sample was concentrated and loaded to a HiLoad 16/600 Superdex 75 column. Peak fractions were pooled, concentrated, frozen in liquid nitrogen, and stored at -80°C.

### *2.2.4 Purification of TEV protease*

A 150 ml overnight culture with ampicillin and chloramphenicol was started from a glycerol stock containing the TEV plasmids pRK793 and pRIL in BL21 (DE3) *E. coli* cells. Six 1 l cultures with an $OD_{600}$ of 0.05 were started and grown at 37°C shaking until an $OD_{600}$ of 0.4 to 0.8 was reached. Cells were induced with 1 mM IPTG and grown for 3 to 6 hours at 30°C. Cells were harvested at 4000 rpm for 20 minutes, pellets were resuspended in lysis buffer (50 mM Tris pH 8.0, 200 mM NaCl, 2 mM BME, 20 mM imidazole), frozen in liquid nitrogen, and stored at -80°C. The pellets were thawed, 60 mg/ml lysozyme, 8 µl benzonase, 2 mM $MgCl_2$, and 2 mM BME were added, and the sample was incubated on ice for 30 minutes, followed by 2 cycles of sonication (2 minutes, 50% power). The sonicated sample was centrifuged at 18000 rpm for 40 minutes at 4°C. The supernatant was filtered with a 45 µm filter. 10 ml of Ni Sepharose 6 Fast Flow beads (GE Healthcare Life Sciences) were equilibrated with lysis buffer, and mixed with the supernatant. The beads were applied to a Gravity Flow Column (Bio Rad) at 4°C and washed with 200 ml of lysis buffer. The protein was eluted with elution buffer (50 mM Tris pH 8.0, 200 mM NaCl, 2 mM BME, 200 mM imidazole) into lysis buffer. The eluate was diluted with buffer (20 mM Tris pH 8.0, 2 mM BME) to 150 mM NaCl and centrifuged at 4500 rpm for 10 minutes. The supernatant was loaded to 2 x 5 ml HiTrap SP FF columns (GE Healthcare Life Sciences) in series at a flow rate of 2 to 3 ml/min. The protein was eluted using gradient elution with buffer (20 mM Tris pH 8.0, 1 M NaCl, 2 mM BME) at a flow rate of 4 ml/min. Peak fractions were pooled, concentrated to 2 mg/ml, frozen in liquid nitrogen, and stored at -80°C.

## 2.3 Nucleotide exchange protocol

This protocol is applicable to HsCdc42, HsRac1, and MBP-Cdc42.
100 µM of the GTPase was incubated for 1 hour shaking at 25°C with 20 µM guanine nucleotide exchange factor (GEF) (Dbs) and 10 mM GMPPNP or GTPγS. Purification of the Dbs GEF was done by other members of the laboratory according to Truebestein et al. (Truebestein et al. 2015). Reaction mixture was loaded onto a HiLoad 10/300 Superdex 75 column (GE Healthcare Life Sciences), peak fractions were pooled, concentrated, and diluted several times with buffer to remove unbound GMPPNP or GTPγS. Protein was frozen in liquid nitrogen, and stored at -80°C.

## 2.4 Verification of the nucleotide exchange

### *2.4.1 by IP-RP HPLC*

Nucleotide exchange was verified by iron-pairing reverse phase HPLC using a Phenomenex C18 column (150 x 4.60 mm, 5 µm, 300 A) with an attached EC 4/3 UNIVERSAL RP guard column (Macherey-Nagel) on an AEKTA Ettan system. A 55 µl loop was used to load the sample (100 µM). Runs were performed in isocratic mode (100 mM KH2PO4/K2HPO4 pH 6.5, 10 mM tetrabutylammonium bromide, 4.5% (v/v) $CH_3CN$) with a flow rate of 1 ml/min. Elution volumes were monitored by absorbance at 280 nm and 260 nm.

### *2.4.2 by mass spectrometry*

Mass spectrometry measurements were done by Dr. Markus Hartl and Dr. Dorothea Anrather of the Mass Spectrometry Facility of the MFPL.
Desalting of protein sample was performed using Micro Bio-Spin™ 6 Columns (Bio Rad) according to manufacturer's protocol. Samples were buffer exchanged with 4 x 500 µl of 50 mM ammonium acetate.

#### *2.4.2.1 Liquid chromatogaphy-mass spectrometry measurement*

Samples were reduced by addition of 10 mM DTT and diluted with 0.1% formic acid to a concentration of 1 ng/µl (Cdc42) or 10 ng/µl (MBP-Cdc42). 10 ng of Cdc42 and 50 ng of MBP-Cdc42 were injected. The peptides were separated on a Dionex 3000 HPLC system using a Aeris™ 3.6 µm WIDEPORE C4 200 Å, LC Column 150 x 2.1 mm (Phenomenex), applying a linear gradient from 5 to 70% solvent B (0.08% formic acid, 90 % CAN; solvent A 0.1 % formic acid) over 10 minutes. Eluting peptides were analyzed on a SynaptG2-Si mass spectrometer in the MS-TOF mode. Survey scans were obtained in a mass range of 600 to 3000 m/z with a scan time of one second in the sensitivity mode.

## 2.5 Lipid binding assay

### *2.5.1 Rhodamine-labeled sucrose-loaded vesicles (SLVs)*

For a final 1 ml of 1 mM total lipid concentration, 50 µl of 20 mg/ml lipids from Folch Fraction 1 were added to 950 µl chloroform, and 0.006 mM rhodamine-DHPE was

added. Lipids were dried to a thin film using a dry nitrogen stream. 1 ml of 20 mM HEPES pH 7.5, 0.3 M sucrose were added and vortexed followed by four cycles of freezing in liquid nitrogen and thawing in sonicating water bath. 300 µl of 20 mM HEPES pH 7.5, 100 mM potassium chloride were added to 250 µl vesicles followed by centrifugation for 30 minutes at 100000 rpm, room temperature in an ultra-centrifuge (TLA 100.1 rotor). Supernatant was removed and the vesicles were resuspended in 20 mM HEPES pH 7.5, 100 mM KCl.

### *2.5.2 Lipid binding assay*

50 µl of SLVs were incubated with 50 µl of 0.2 mg/ml CeMRCK1 955-1592 for 20 minutes at room temperature. The sample was centrifuged for 20 minutes at 30000 rpm (ultra-centrifuge) and supernatant and pellet fractions were loaded on a 10% SDS-PAGE gel.

## 2.6 Complex formation between CeMRCK1 and Cdc42

### *2.6.1 Analytical gel filtration of Cdc42 and MRCK1*

CeMRCK1 955-1592 was incubated with a threefold excess of Cdc42.GMPPNP for 1 hour to allow complex formation. Samples of Cdc42.GMPPNP, CeMRCK1 955-1592, and the reaction mixture were applied to a Superdex 200 Increase 10/300 GL column (GE Healthcare Life Sciences) equilibrated in 20 mM Tris pH 7.5, 150 mM KCl, 1 mM TCEP, 1% glycerol.

### *2.6.2 Cdc42-CRIB binding assay*

Cell pellet of the GST-tagged CRIB peptide was thawed; 1 mM benzamidine, 2 µl benzonase, and 0.2 mg/ml lysozyme were added, and left for 30 minutes on ice. The whole cell lysate was sonicated three times for one minute, followed by centrifugation for 30 minutes at 18000 rpm, 4°C. Supernatant was incubated with washed and equilibrated Glutathione Sepharose 4B beads (GE Healthcare Life Sciences) for 2 hours at 4°C. Beads were spun down for 7 minutes at 700 x g and the beads were washed four times with buffer (50 mM Tris pH 7.4, 150 mM KCl, 2 mM $MgCl_2$, 1 mM TCEP). To test whether Cdc42 is binding to the CRIB peptide, 40 µl beads were incubated with 20 µl of 200 µM Cdc42.GMPPNP and 140 µl buffer rotating for 30 minutes at room temperature. After a sample was taken, the beads were centrifuged

for 5 minutes at 700 x g. A sample of the supernatant was taken before it was discarded; a sample of the beads was taken after resuspension in 200 µl buffer. These steps were repeated two more times. As a control, GST loaded beads were treated exactly the same way as the GST-CRIB loaded ones. Samples of supernatant and pellet fractions were loaded on a 12% SDS-PAGE gel.

### *2.6.3 Fluorescence anisotropy assay*

Binding affinities of Cdc42, MBP-Cdc42, or Rac1 for FITC-labeled CRIB peptide (QISTPSDFMHIVHMGPAPVMELQQNFIDLQ, GenScript) were measured by fluorescence anisotropy. 500 nM of FITC-labeled CRIB peptide was prepared and the GTPase was titrated to this solution in increasing concentrations (100 nM to 60 µM). Fluorescence anisotropy was measured in a Perkin Elmer LS50B fluorimeter ($\lambda_{ex}$ = 498 nm, $\lambda_{em}$ = 518 nm) at 20°C.

## 2.7 Crystallization of CeMRCK1 regulatory region

### *2.7.1 Limited proteolysis with trypsin and chymotrypsin of CeMRCK1 955-1592*

2.5 µM of protein was incubated with 1.4 µM of protease (1 mg/ml protease stock diluted 1:30 with gel filtration buffer (20 mM Tris pH 7.5, 150 mM KCl, 1 mM TCEP, 1% glycerol)) at room temperature. Samples were taken after 0, 10, 20, 30, 60, 90, 120 and 180 minutes. Samples were loaded to 12% SDS PAGE gel. For subsequent limited proteolysis reactions of CeMRCK1 955-1592, 2.5 µM protein was incubated with 1.4 µM protease for 10 minutes and reaction was stopped by adding 100 µM PMSF. The sample was concentrated and loaded to a HiLoad 10/300 Superdex 75 column (GE Healthcare Life Sciences). Peak fractions were pooled and concentrated. The protein was frozen in liquid nitrogen and stored at -80°C.

### *2.7.2 Crystallization trials*

In order to crystallize the CeMRCK1 955-1592 construct, initial crystal screens were set up using the Phoenix Crystallization Robot (Art Robbins Instruments) or the Oryx Protein crystallization Robot (Douglas Instruments Ltd): JCSG-plus screen (Molecular Dimensions), Morpheus screen (Molecular Dimensions), MIDAS (Molecular Dimensions) and Crystal Screen HT (Hampton Research). For crystallization trials of the CeMRCK1 955-1517 Crystal Screen HT (Hampton

Research), JBScreen Classic (Jena Bioscience), Morpheus (Molecular Dimensions), JCSG Plus Screen (Molecular Dimensions), and PEG/Ion HT Screen (Hampton Research) were used. In each screen, drops with protein to reservoir solution ratios of 1:1 (200 µl + 200 µl) and 2:1 (400 µl + 200 µl) were set up.

### *2.7.3 Microseeding*

Sead Bead (Hampton Research) was used to create a seed stock according to manufacturer's protocol. Crystals were crushed with a pipette and together with 10 µl reservoir solution transferred to the Sead Bead tube (on ice). This was repeated for times until no crystal remained in the plate (final volume in the Sead Bead Tube: 50 µl). Sead Bead Tubes were vortexed 4 to 5 times for 30 seconds, allowing them to cool on ice between every vortexing step. For serial dilution, 45 µl of reservoir solution were mixed with this seed stock to obtain a $10^{-1}$ dilution. From this again 5 µl were diluted with 45 µl reservoir. In this manner dilutions of $10^{-1}$ to $10^{-8}$ were obtained. These seed stock dilutions were used to set up crystallization drops containing 1 µl protein, 1 µl reservoir solution, and 0.3 µl microseeds or 1.5 µl protein, 0.75 µl reservoir solution, and 0.35 µl microseeds for 1:1 or 2:1 protein to reservoir solution ratio, respectively.

## 2.8 X-ray diffraction data collection

Diffraction data was collected on ID-29 at the European Synchrotron Radiation Facility in Grenoble, France. Crystals diffracted to 2.3 Å and belong to space group P1, with unit cell dimensions of a = 69.25 Å, b = 98.05 Å, c = 131.66 Å, α = 81.47°, β = 77.75°, γ = 80.46°. A native dataset was collected to 2.3 Å, but efforts to solve the structure by molecular replacement failed. Experimental phases will hopefully be obtained from crystals of selenomethionine-substituted protein. A Matthews analysis indicated the presence of 5 or 6 molecules per asymmetric unit, and strong six-fold rotational symmetry in the self-rotation function would suggest it is actually 6.

# 3 RESULTS

## 3.1 Purification of a regulatory domain construct of MRCK

No studies to date have explicitly addressed the role of the C-terminal regulatory domains of MRCK and its contribution in membrane targeting. The C-terminal region contains the phorbol ester interacting C1 domain, the citron homology (CNH) domain, the pleckstrin homology (PH) domain, and the Cdc42-binding CRIB domain (Figure 1). Previous attempts in our laboratory to purify the CNH domain alone resulted in soluble aggregates but a construct containing the C1, the PH, and the CNH domain could be purified as a single construct to homogeneity (data not shown). This led to the assumption that these three domains may act in concert in targeting MRCK to the membrane and its substrates. A construct containing residues 955-1534 could be crystallized but the protein crystals could not be optimized for the collection of X-ray diffraction data. Since Cdc42 is an important factor contributing to MRCK's functioning in the cell, we also purified the whole C-terminal region including the Cdc42-binding CRIB domain.

The CeMRCK1 955-1592 construct with an N-terminal $His_{10}$ - affinity tag and a TEV cleavage site for removal of the tag was previously cloned and expressed in Sf9 insect cells from other members of the laboratory (Figure 1 b). For purification, the protein solution was applied to an immobilized metal ion affinity chromatography column (Ni-NTA matrix) to isolate the overexpressed polyhistidine-tagged protein from the cell lysate. The protein interacts via the $His_{10}$ tag with the metal ions in the column and is retained on the column. The protein was eluted from the column by gradient elution with imidazole. The peak fractions were checked via SDS-PAGE to ensure successful overexpression and isolation of the protein (Figure 2 a). The 955-1592 construct of CeMRCK1 has a size of approximately 72 kDa, a value that fits well with the bands on the gel after the first purification round. To prepare the sample for crystallization and to avoid interference of the tags in downstream assays, the $His_{10}$ - affinity tag was removed by overnight digestion with TEV protease. The protein sample was then loaded to a cation exchange column to remove the protease and other contaminating proteins (Figure 2 b). Finally, gel filtration was performed and the peak fractions were checked on a SDS-PAGE gel (Figure 2 c). The elution

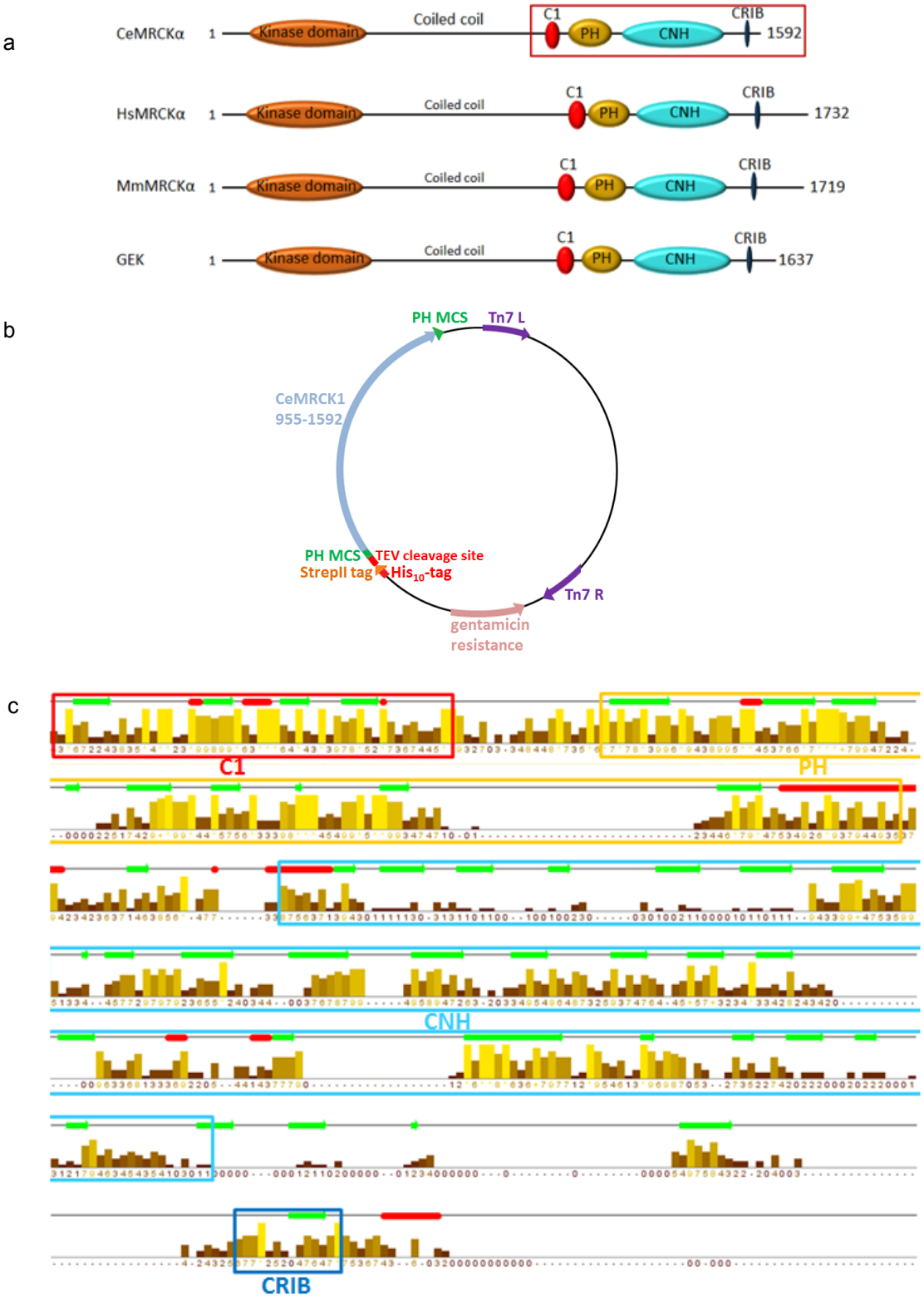


**Figure 1 MRCK kinases and their regulatory domains** a) domain organization of the C. elegans, the human, the mouse and the *D. melanogaster* MRCK isoforms b) schematic construct of the pFastBac plasmid with the CeMRCK1 955-1592 construct, and with TEV cleavage site, $His_{10}$-tag, PH multiple cloning sites (MCS), Mini Tn7 elements, gentamicin resistance cassette, StrepII tag c) alignment of ancestral orthologues of MRCK and secondary structure prediction

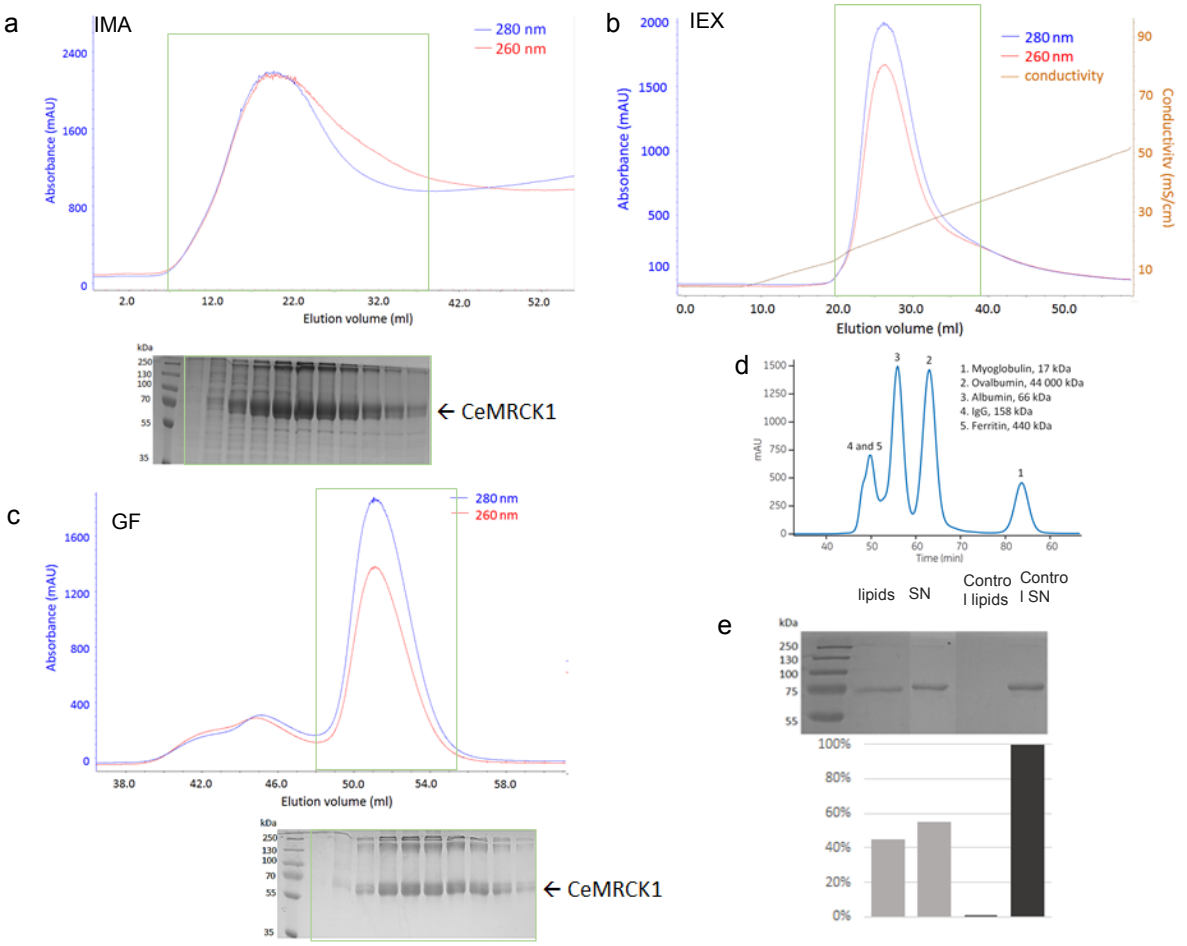


**Figure 2 Purification of CeMRCK1 955-1592 and lipid binding assay** a) elution profile of IMAC, peak fractions loaded to a 12% SDS-PAGE gel b) elution profile of cation exchange chromatography (IEX) c) elution profile of final gel filtration (GF), peak fractions loaded to 12% SDS-PAGE gel d) elution profile of a protein standard mix on HiLoad 16/600 Superdex 75 prepgrade column e) liposome binding assay of CeMRCK1 955-1592 construct, 45% is binding to liposomes; control experiment was done without protein; SN = supernatant

volume of the peak fits well with a size of approximately 70 kDa, when compared to the elution peaks of the standard protein mix (Figure 2 d), indicating that the protein behaves as a monomer. Coomassie staining of the peak fractions indicated a highly pure preparation. The protein sample was concentrated to 4 mg/ml.

## 3.2 Binding assay of MRCK to lipids

MRCK has been shown to be ubiquitously expressed with highest expression in the brain (Leung et al. 1998). In the absence of known lipid ligands for the C1, PH, and CNH domain, we therefore tested binding of MRCK to brain lipids. Folch Fraction 1, a brain extract from bovine brain containing phophatidylinositols, phosphatidylserine

and other brain lipids was used to mimic membranes. The purified CeMRCK1 construct was incubated with sucrose-loaded vesicles (SLVs) containing Folch fraction 1. After centrifugation, binding of the protein to the lipids was checked via SDS-PAGE (Figure 2 e). A control experiment was done in parallel without any protein. Evaluation of the bands on the gel revealed that approximately 45% of CeMRCK1 955-1592 is binding to lipids, whereas the other 55% are unbound in the supernatant.

## 3.3 Limited proteolysis, protein crystallization, and diffraction data collection

In order to understand the function of the C-terminal regulatory domain better, attempts were made to crystallize and solve the structure of the CeMRCK1 955-1592 construct. Since no protein crystals could be obtained with different commercial crystal screens, the protein was incubated with trypsin or chymotrypsin to identify flexible or labile regions in the protein. To test whether proteolysis with these enzymes yielded stable protein constructs, the protein was incubated with each protease for a total of 180 minutes and samples were taken at regular time intervals to test stability of the protein. Limited proteolysis occurred immediately after addition of either protease but the proteolysed construct remained stable after three hours (Figure 3 a) and even overnight (data not shown). After these first trials, for all following proteolysis reactions the protein was incubated for ten minutes with the protease, reaction was stopped by adding PMSF, a protease inhibitor, and the sample was loaded to a gel filtration column to get a protein of high enough purity for crystallization (Figure 3 b). In order to determine the mass, and thereby the sequence of the trypsin-treated construct, a sample was prepared for mass spectrometry. Intact mass determination yielded a mass of 62982.3 Da (Figure 3 g), which is best fit by amino acids 955 to 1517 with an expected mass of 62971.3 Da. This construct would be compatible with trypsin cleavage, since residue 1517 is a lysine.

Crystallization trials with both trypsin and chymotrypsin-treated proteins yielded crystals in the Morpheus Screen (Figure 3 c and d). Initial crystals grew in conditions C1, C9, D9, E5, E9, and G1 (see Table 2). Crystals of the trypsin-treated protein looked more promising than those of the chymotrypsin-treated ones and so optimization of the crystals was performed using the trypsin-treated CeMRCK1 955-

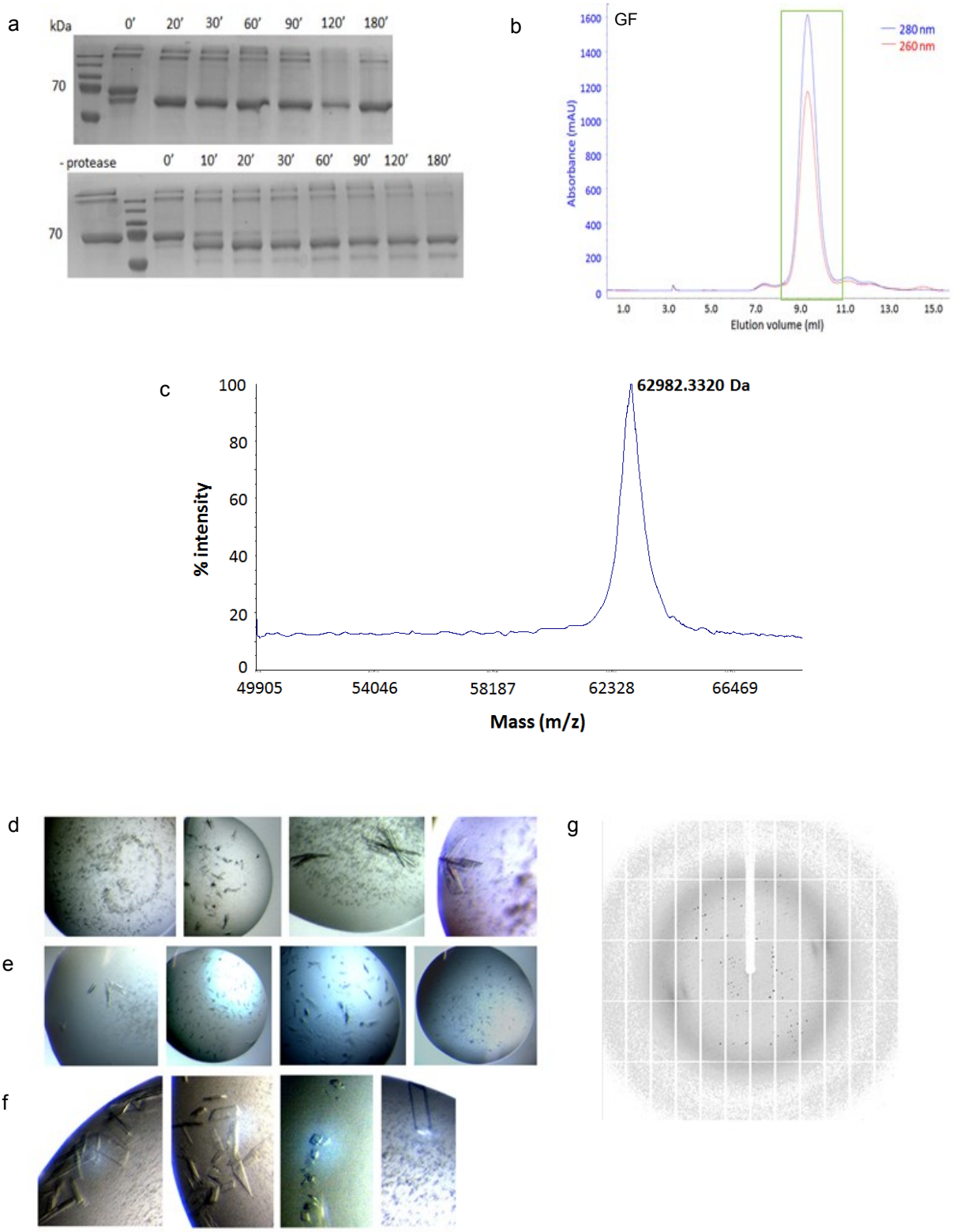


**Figure 3 Limited proteolysis, crystallization and diffraction data** a) Limited proteolysis assay of CeMRCK1 955-1592 with trypsin (on top) and chymotrypsin (below) for up to 180 minutes, samples were taken in regular time intervals b) elution profile of gel filtration after proteolysis reaction c) MS spectrum d) initial protein crystals of the trypsin proteolysed (Morpheus screen conditions C1, C9, D9, E9) and e) the chymotrypsin proteolysed construct (Morpheus screen conditions C1, C9, G5, G9) f) optimized protein crystals g) diffraction data

1592 construct. For every crystallization screen, protein drops with protein to reservoir solution ratios of 1:1 and 2:1 were set up. The most promising crystals were obtained in conditions C1 and E9 (see Table 2). Optimization steps to overcome high nucleation and clustering of the protein crystals were mainly performed by Dr. Linda Trübestein and included screening of precipitant concentration, screening for additives, growing crystals at 4°C instead of 20°C, microseeding, streak seeding with a horsehair and filtering of the protein. These optimization steps yielded crystals (Figure 3 e) that could be harvested and sent to the European Synchrotron Radiation Facility (ESRF) in Grenoble. Optimized conditions for these crystals were: Buffer system 3 pH 8.5, 0.09 M NPS, 20% P550MME, 8% P20K, 3 – 5% Glycerol and Buffer system 3 pH 8.5, 0.09 M NPS, 18% P550MME, 10% P20K, 10 mM DTT. The protein crystals diffracted to 2.3 Å (Figure 3 f), with space group P1 and six molecules per asymmetric unit. A native dataset was collected to 2.3 Å and is summarized in Table 1. Attempts to solve the structure by molecular replacement with homologous structures of the PH and C1 domains failed.

| **Data collection** | |
|---|---|
| Space group | P1 |
| Unit cell (a, b, c in Å) | 69.15, 97.49, 131.44 |
| Unit cell (α, β, γ in °) | 81.37, 77.76, 80.40 |
| Resolution range (Å) | 59 – 2.37 |
| Observations | 767,133 |
| Unique reflections | 228,685 |
| Completeness (%) | 94.3 (90.6) |
| Multiplicity | 3.4 |
| $R_{pim}$ | 0.068 (0.483) |
| I/σ(I) | 8.0 (1.6) |
| CC(1/2) | 0.994 (0.672) |

**Table 1 Dataset statistics table** for protein crystals of the trypsin treated CeMRCK1 955-1592 construct

## 3.4 Selenomethionine-substituted protein expression, purification, and crystallization of CeMRCK1 955-1517

In order to obtain experimental phases with which to solve the structure, selenomethionine substituted CeMRCK1 955-1592 was expressed and purified from Sf9 cells. Cells were grown in methionine deficient medium for three passages before they were infected with recombinant baculovirus and supplemented with selenomethionine. The protein was purified according to the purification protocol of the native CeMRCK1 955-1592 construct (Figure 4 a and b). The protein sample was treated with trypsin after cation exchange chromatography. Unfortunately, during cation exchange chromatography, the UV lamp broke and the purification had to be continued “blindly”. The elution peak was estimated according to purification of the normal protein and the conductivity, and was checked on a 10% SDS PAGE gel (Figure 4 b). The protein was concentrated and diluted several times to remove the protease and to exchange the protein into a suitable buffer for crystallization. Final protein yield was 100 µl of 2.82 mg/ml (45 µM). Unfortunately, due to problems with the crystallization robot, all of this selenomethionine-substituted protein was lost when setting up the first crystal plate. Since the yield of the selenomethionine-substituted protein was significantly lower than of the native protein, it was important to avoid the proteolysis step.

Based on mass spectrometry analysis of the trypsin-cleaved protein (Figure 3 c), construct of CeMRCK1 comprising amino acids 955-1517 was cloned. CeMRCK1 955-1517 was expressed and purified from recombinant baculovirus-infected Sf9 cells according to the protocol for the 955-1592 construct: immobilized metal ion affinity chromatography was followed by TEV cleavage of the $His_{10}$-tag overnight, followed by cation exchange chromatography and gel filtration. Purification was checked via SDS-PAGE (Figure 4 d to f). The purified protein was used to set up the Morpheus crystallization screen. Crystals grew in conditions C9, D9, E9, and F9 (Table 2) similar to those conditions of the crystals from the trypsin-treated 955-1592 construct. All of these crystals grew in drops with a protein to reservoir solution of 2:1. In order to get bigger and more regular crystals, optimization was done using different precipitant concentrations, microseeding, streak seeding with a horsehair, addition of different concentrations of glycerol, 1,4-dithiothreitol, ammonium sulfate,

butanol, and dimethyl sulfoxide, growing crystals at 4°C, as well as combinations of these methods. Varying precipitant concentration and the concentration of alcohols for D9, in combination with microseeding led to bigger crystals. Streak seeding with a horse hair led to crystals in only one drop. Best crystals were obtained in condition D9 (see Table 1) with 0.1 M alcohols, 6 % glycerol, $10^{-1}$ seed stock, and 1:1 protein to reservoir ratio; condition D9 with 0.1 M alcohols, 2% ethanol, $10^{-1}$ seed stock, and 2:1 protein to reservoir ratio; condition F9 with 12% P550MME, 18% P20K, 8% glycerol, $10^{-1}$ seed stock, and 2:1 protein to reservoir ratio; and condition F9 with 12% P550MME, 18% P20K, streak seeding (Figure 4 g left to right). Expression of selenomethionine-substituted CeMRCK1 955-1517 is currently in progress, but if diffraction-quality crystals can be obtained from this protein, it is hoped that experimental phases can be collected and the structure solved.

## 3.5 Cdc42 – purification and interaction with MRCK

For the experiments with Cdc42, we worked with the human homologue. Between the human and the *C. elegans* Cdc42 there are only seven amino acid substitutions (Figure 5 a) that are not involved in effector binding. Because of this, we were confident that both proteins would behave in the same manner and that binding of HsCdc42 to CeMRCK1 would not differ from binding of CeCdc42 to the kinase. The cysteine of the C-terminal CAAX box of Cdc42 is prenylated with a geranylgeranyl moiety, which is responsible for attachment to the membrane (Johnson 1999). To be

| | Buffer system | pH @ 20°C | Additives | Precipitants |
|---|---|---|---|---|
| C1 | 1 | 6,5 | 0,09M NPS | 30% P550MME_P20K |
| C9 | 3 | 8,5 | 0,09M NPS | 30% P550MME_P20K |
| D9 | 3 | 8,5 | 0,12M alcohols | 30% P550MME_P20K |
| E5 | 2 | 7,5 | 0,12M ethylene glycols | 30% P550MME_P20K |
| E9 | 3 | 8,5 | 0,12M ethylene glycols | 30% P550MME_P20K |
| F9 | 3 | 8,5 | 0,12M monosaccharides | 30% P550MME_P20K |
| G1 | 1 | 6,5 | 0,1M carboxylic acids | 30% P550MME_P20K |

**Table 2 Morpheus Crystal Screen Conditions that yielded crystal growth.** Buffer system 1 (Imidazole; MES monohydrate (acid)), Buffer system 2 (Sodium HEPES; MOPS (acid)), Buffer system 3 (Tris (base); BICINE); 20% P550MME, 10% P20K

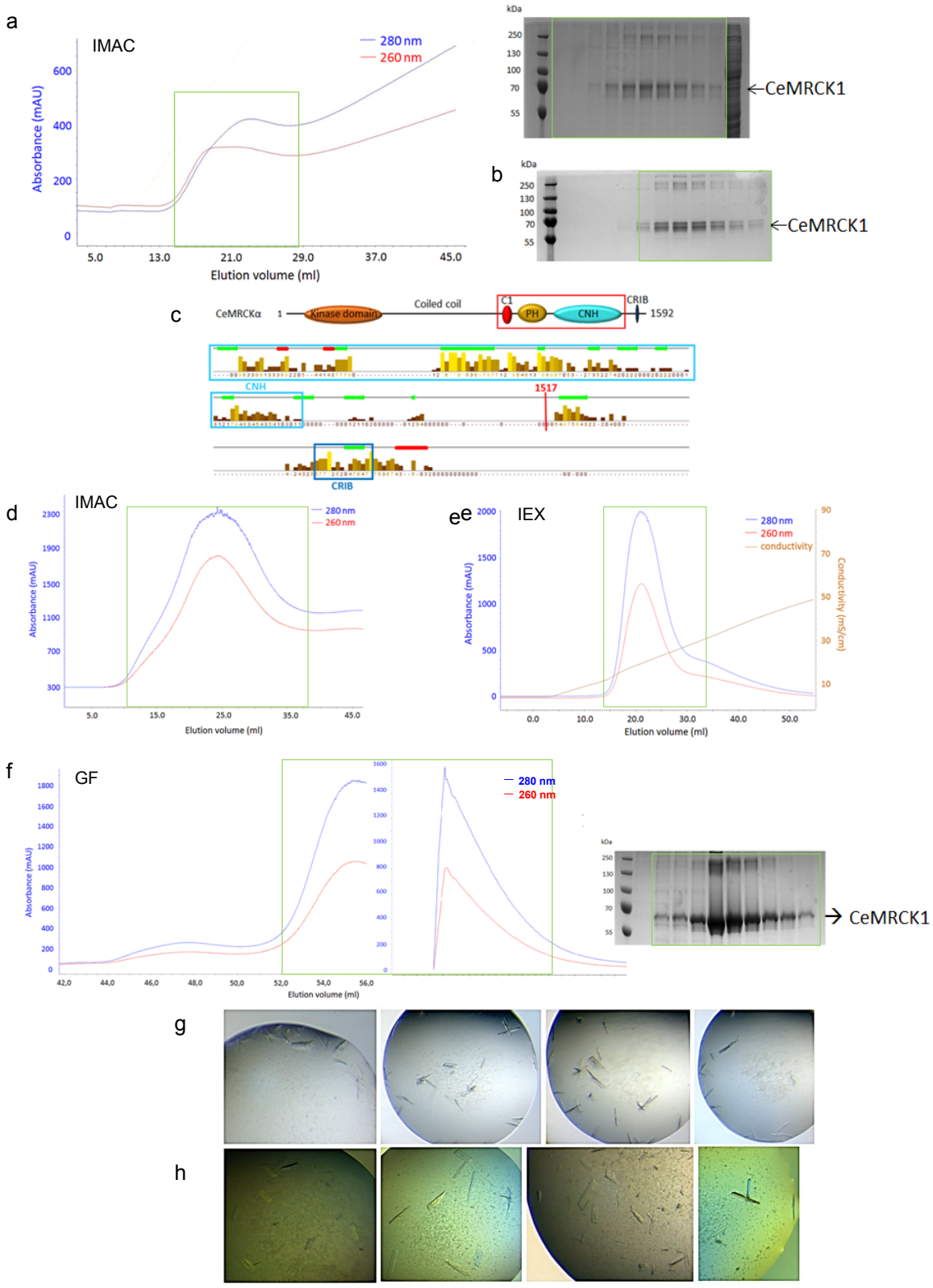


**Figure 4 Purification of selenomethionine-substituted protein, purification and crystallization of CeMRCK1 955-1517** a) and b) purification of selenomethionine-substituted CeMRCK1 955-1592 a) elution profile of IMAC and peak fractions loaded to 12% SDS-PAGE gel b) peak fractions of cation exchange chromatography fractions loaded to 12% SDS-PAGE gel c) domain organization of CeMRCK1 and secondary structure prediction/conservation of region around amino acid 1517 d) to f) purification of CeMRCK1 955-1517 construct d) elution profile of IMAC e) elution profile of cation exchange chromatography (IEX) f) elution profile of gel filtration (GF) and peak fractions loaded to 12% SDS-PAGE gel g) initial crystals (Morpheus screen conditions C9, D9, E9, F9) h) optimized crystals

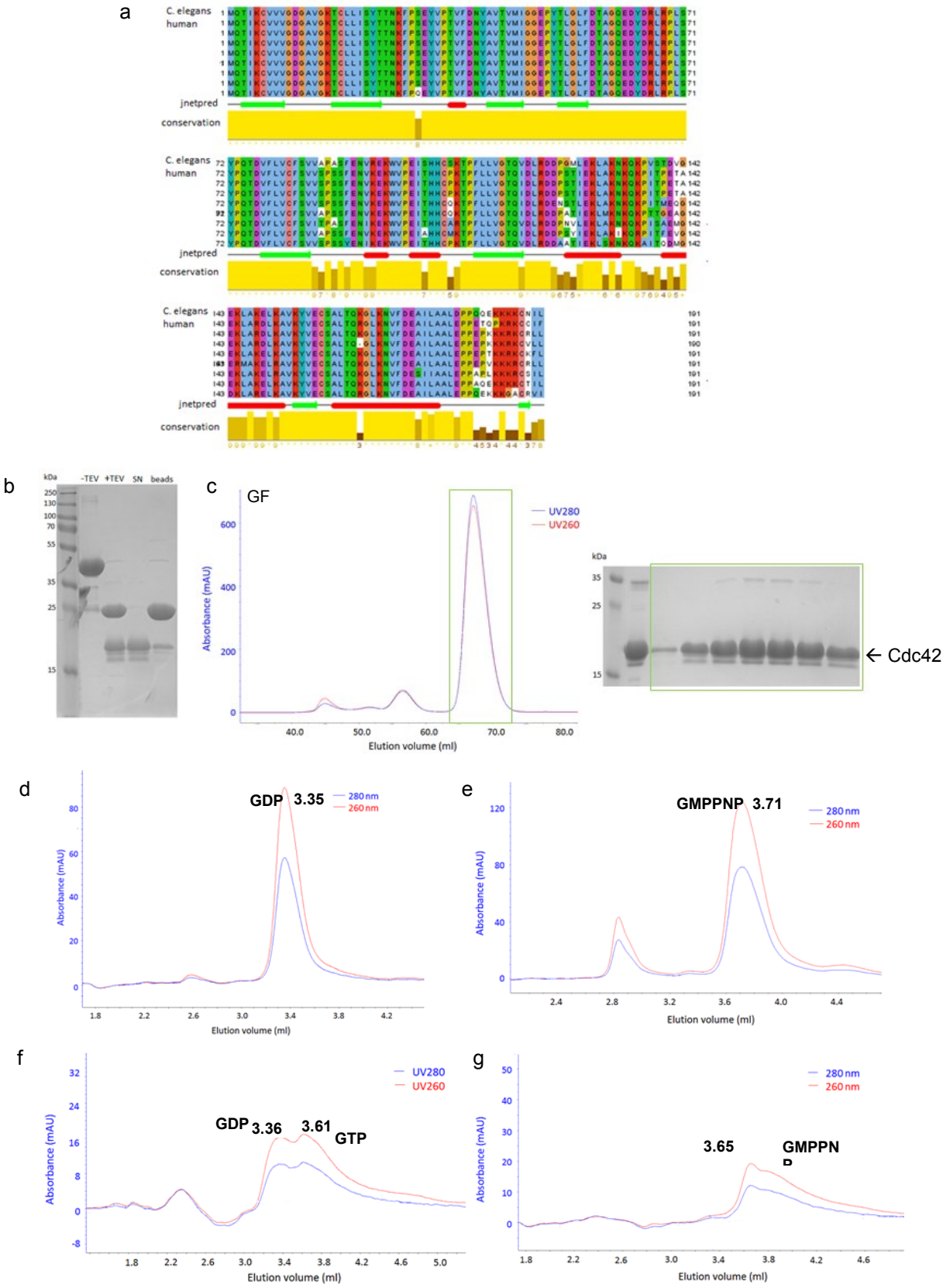
a
C. elegans
human
jnetpred
conservation
b
kDa
-TEV +TEV SN beads
c
GF
UV280
UV260
Absorbance (mAU)
Elution volume (ml)
kDa
← Cdc42
d
GDP 3.35
280 nm
260 nm
e
GMPPNP 3.71
f
GDP 3.36
3.61
GTP
g
3.65
GMPPN

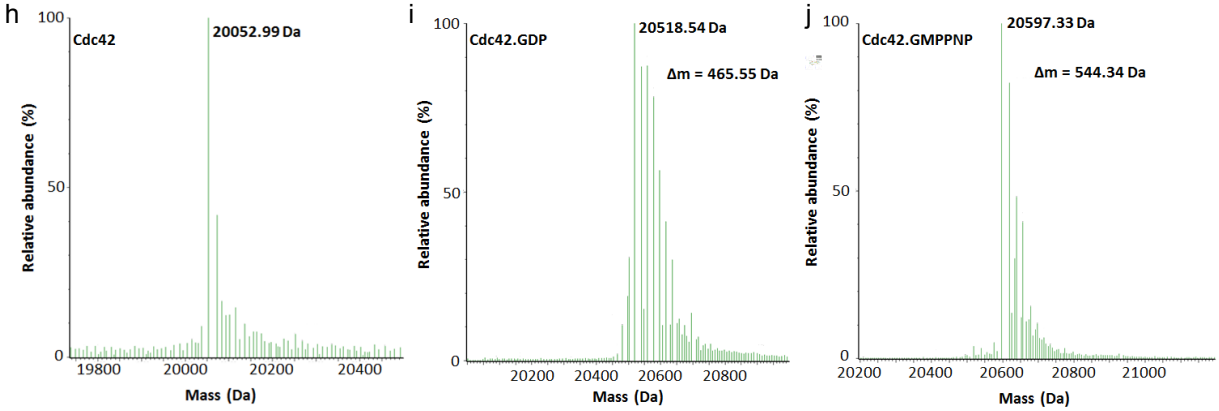


**Figure 5 Purification and nucleotide exchange of HsCdc42** a) Alignment of ancestral Cdc42 orthologues and secondary structure prediction b) and c) purification of Cdc42 b) Cdc42 isolation via binding to glutathione sepharose beads before (-TEV) and after (+TEV) cleavage from the beads and purification from the beads via centrifugation (SN), 12% SDS-PAGE gel c) elution profile of gel filtration and peak fractions loaded to 12% SDS-PAGE gel d) to g) verification of nucleotide exchange via HPLC d) elution profile of GDP e) of GMPPNP f) elution profile of purified Cdc42 and g) of GMPPNP exchanged Cdc42 h) to j) mass spectrometry data for Cdc42 h) deconvoluted spectrum from charge states in m/z range: 813-923 from LC-MS, denaturing condition; mass for Cdc42 is measured to be 20052.99 Da (calculated 20054.1 Da) i) deconvoluted spectrum from native MS for purified Cdc42, mass difference between empty (denatured) Cdc42 and native, purified Cdc42 of 465.55 Da fits mass of GDP and bound $Mg^{2+}$ (calculated 465.32 Da) j) deconvoluted spectrum from native MS for GMPPNP exchanged Cdc42, mass difference between empty (denatured) Cdc42 and native Cdc42.GMPPNP of 544.34 Da fits mass of GMPPNP and bound $Mg^{2+}$ (calculated 544.32 Da)

able to purify the soluble Cdc42 protein we cloned a construct missing this C-terminal CAAX box. Amino acids 2-178 of HsCdc42 were cloned into pGST parallel and expressed in *E. coli* as GST fusion protein with a TEV cleavage site for removal of the GST tag. Purification was accomplished by affinity chromatography, using glutathione sepharose beads to which the protein was bound via its GST-tag (Figure 5 b). HsCdc42 was cleaved on the beads using TEV protease before the protein was loaded to a gel filtration column. Presence and purity of the protein was checked via SDS PAGE (Figure 5 c). Due to the relatively fast intrinsic GTP hydrolysis rate of Cdc42 (Zhang et al. 1997), GTP had to be exchanged for a non-hydrolysable analogue to ensure the active state of the GTPase. The nucleotide exchange reaction was accomplished in the presence of the Dbs exchange factor (Truebestein et al. 2015), Dbs was removed from the sample via gel filtration, and the exchange was verified by ion-pairing reverse-phase (IP-RP) HPLC and mass spectrometry. The IR-RP HPLC was calibrated with standards of GDP and GMPPNP (or GTPγS). For GDP, the peak maximum was at an elution volume of 3.35 ml (Figure 5 d), whereas GMPPNP eluted at 3.71 ml (Figure 5e). The purified Cdc42 showed two peaks, one peak at 3.36 ml and the other at 3.61 ml (Figure 5 f). For the GMP-PNP loaded

sample the peak maximum was at 3.65 ml (Figure 5 g). This data indicates that the exchange reaction was successful. To further verify the exchange reaction, we prepared a sample of the purified and the exchanged protein for mass spectrometry. The protein sample was desalted into 50 mM ammonium acetate according to manufacturer's protocol using Micro Bio-Spin™ 6 Columns (Bio Rad). Figure 5 h to j shows the results of the mass spectrometry measurements. The shift in mass between the unloaded and the purified Cdc42 and between the unloaded and the exchanged Cdc42 corresponds exactly to the mass of GDP and GMPPNP, respectively. The data for the purified protein shows a second peak that could be derived from GTP, but due to salt adducts this second peak is difficult to interpret. Together, the IP-RP HPLC and MS data confirm the successful exchange reaction. To establish whether GMPPNP-loaded Cdc42 could form a stable complex with CeMRCK1, we first incubated Cdc42 with CeMRCK1 955-1592, a construct of MRCK1 containing the CRIB motif. The protein mixture was applied to an analytical gel filtration column, after initial runs with each protein separately. The peak maxima for Cdc42 and CeMRCK1 955-1592 were at an elution volume of 1.91 ml and 1.65 ml, respectively (Figure 6 a and b). Size exclusion of the mixture of Cdc42 and CeMRCK1 955-1592 yielded two separate peaks with their maxima at 1.63 ml and 1.91 ml (Figure 6 c). This suggests that the affinity of the two proteins for each other is too low to be detected by size exclusion chromatography.

To determine binding of Cdc42 to the CeMRCK1 CRIB in solution, a pull-down binding assay with the extended CRIB domain of CeMRCK1 was performed. The alignment to other Cdc42 isoforms and the chosen sequence of the extended CRIB peptide are shown in Figure 6 d. For this assay the GST-tagged CRIB peptide was cloned and expressed in *E. coli*. The CRIB peptide was bound to glutathione sepharose beads via its GST-tag. The beads with the bound peptide were further incubated with Cdc42.GMPPNP. After centrifugation, the supernatant and the bead fractions were investigated by SDS PAGE. If Cdc42 bound the CRIB peptide, it should be found in the pellet fraction with the peptide bound to the beads, if the GTPase did not bind to the peptide, it should be found in the supernatant. As a control, beads were used that had only GST but no peptide bound. In the control reaction as well as in the actual binding assay, Cdc42 was only found in the

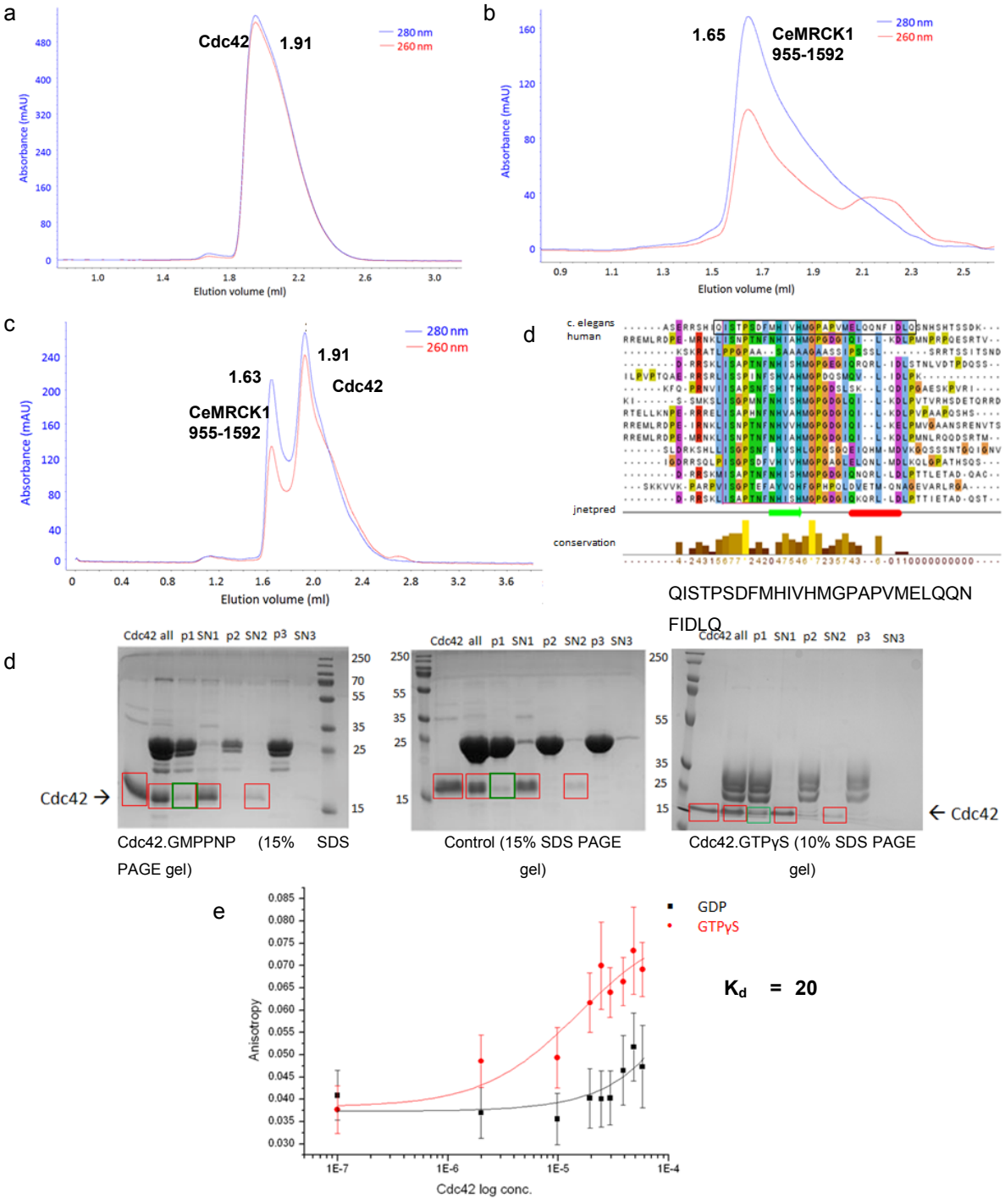


**Figure 6 Binding assays of Cdc42 to MRCK** a) to c) verification of binding of Cdc42.GMPPNP to CeMRCK1 955-1592 via gel filtration a) Cdc42.GMPPNP b) CeMRCK1 955-1592 c) CeMRCK1 955-1592 + Cdc42.GMPPNP d) alignment of CRIB region in ancestral orthologues of MRCK, CRIB peptide: QISTPSDFMHIVHMGAPVMELQQNFIDLQ e) to g) binding assay of Cdc42 to CRIB peptide, Cdc42.GMPPNP and control loaded to 15% gel, Cdc42.GTPγS loaded to 10% gel e) Cdc42.GMPPNP f) control (GST bound to beads) g) Cdc42.GTPγS h) anisotropy assay, $K_d$ = 20 µM

supernatant (Figure 6 e, f, g, red rectangles). In the first pellet fraction (Figure 6 e, f, g, green rectangles) a faint band can be seen in both the control assay as well as in the actual binding assay but is lost after one washing step. In this experiment we could not detect any binding of Cdc42 to the GST-CRIB peptide immobilized on the beads. The experiment was also repeated with Cdc42-GTPγS (Figure 6 g) but no changes could be observed. This experiment again suggests no binding of Cdc42 to the CRIB domain of MRCK1.

Since both size exclusion chromatography and pull-down assays cannot detect low affinity interactions, we next investigated the binding by solution fluorescence anisotropy. We obtained a peptide (amino acids 1543 to 1572 of CeMRCK1 5'-QISTPSDFMHIVHMGPAPVMELQQNFIDLQ-3') labeled with the fluorescent dye fluorescein isothiocyanate (FITC) from GenScript. We titrated increasing amounts of either Cdc42-GDP or Cdc42-GTPγS into a solution of 500 nM FITC-labeled CRIB peptide and recorded the change in anisotropy. Although the changes in anisotropy were not big, ranging from ~0,04 to ~0,07 for Cdc42-GTPγS, compared to the inactive Cdc42.GDP the active Cdc42.GTPγS led to concentration- dependent changes in anisotropy that might reflect the binding of Cdc42 to the CRIB peptide with an estimated $K_d$ of 20 µM (Figure 6 h). This increase in anisotropy was not detected with the GDP-bound Cdc42, but saturation of the binding curve was not achieved and the curve is noisy due to the very small changes in anisotropy. To better evaluate binding by fluorescence anisotropy, we cloned, expressed, and purified Cdc42 fused to MBP at its N-terminus. The increased size of the fusion protein with respect to Cdc42 alone (60 kDa compared with 20 kDa) was expected to increase the concentration dependent change in anisotropy in response to binding to the CRIB peptide. The fusion protein was purified from the cell lysate via its N-terminal $His_6$-tag (Figure 7 a). The polyhistidine tag was cleaved off overnight by TEV protease and removed from the sample afterwards by gel filtration (Figure 7 b). MBP-Cdc42 was loaded with GMPPNP according to the same protocol as for Cdc42. After the nucleotide exchange reaction, the Dbs exchange factor was removed via its histidine tag on an IMAC column (Figure 7 c). The successful exchange reaction was verified by ion-pairing reverse-phase HPLC and mass spectrometry (Figure 7 d to j). The purified MBP-Cdc42 protein showed an elution maximum at 3.23 ml (Figure 7 f) compared to GDP eluting at 3.22 ml (Figure 7 d). The GMPPNP exchanged protein

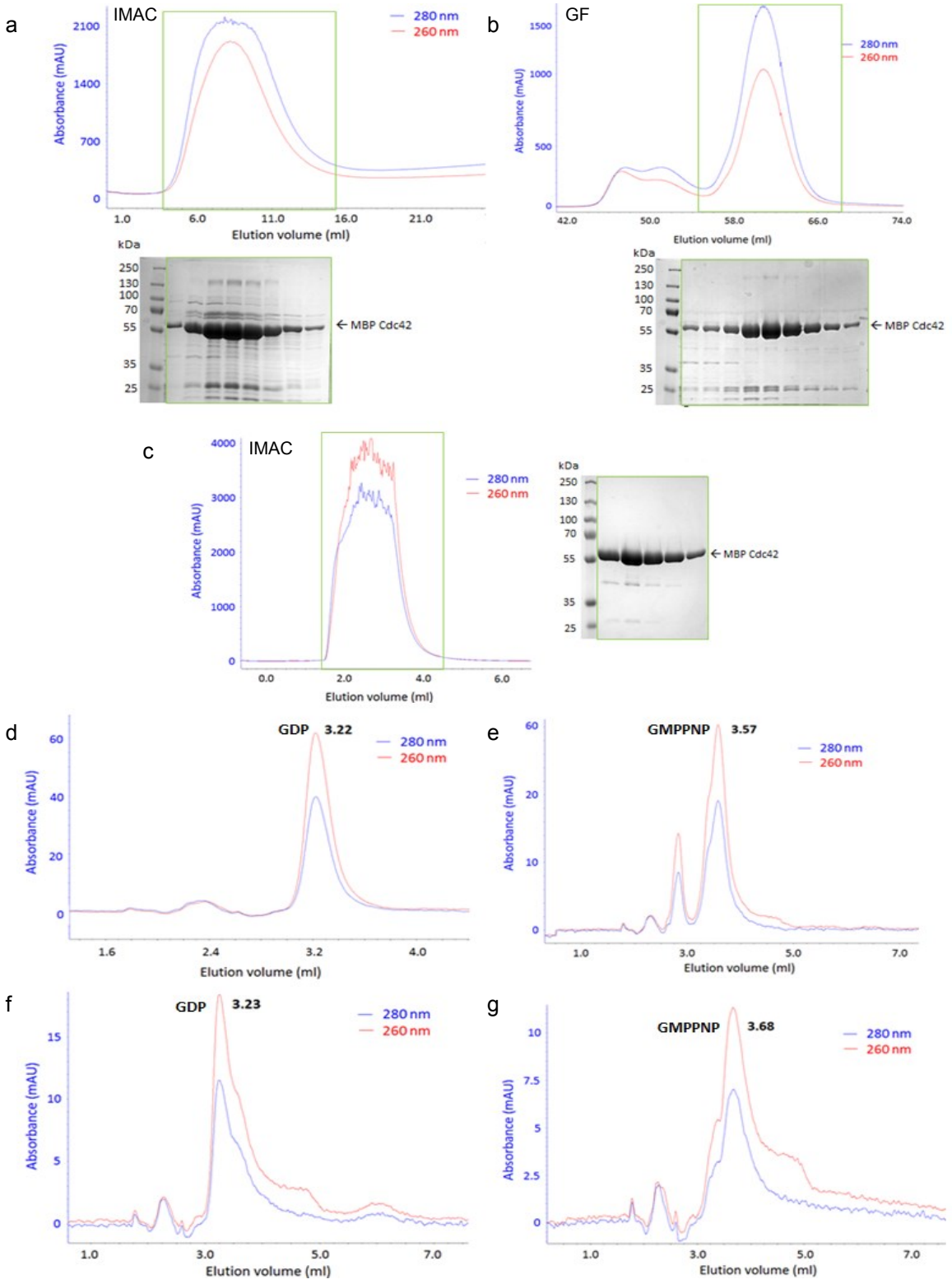
a
IMAC
280 nm
260 nm
Absorbance (mAU)
Elution volume (ml)
kDa
MBP Cdc42
b
GF
c
IMAC
d
GDP 3.22
e
GMPPNP 3.57
f
GDP 3.23
g
GMPPNP 3.68

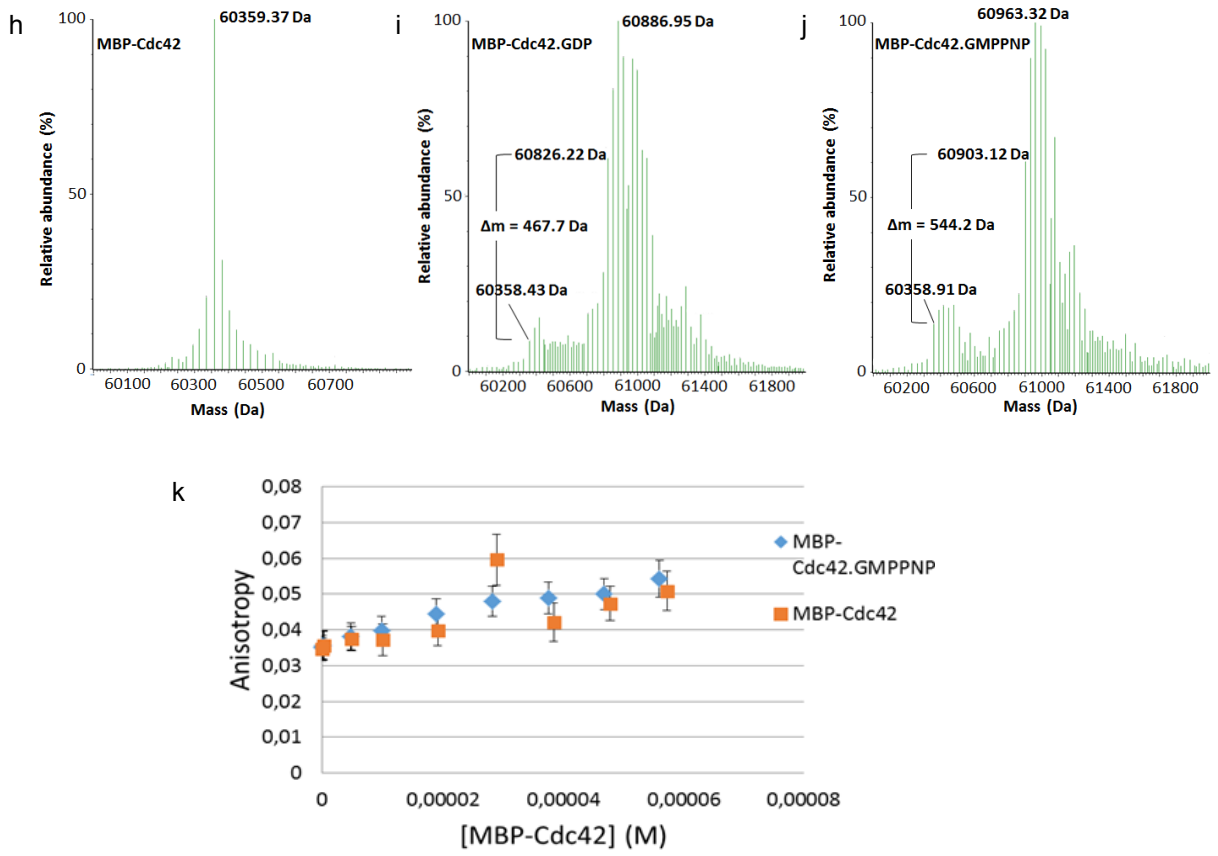


**Figure 7 MBP-Cdc42 purification, nucleotide exchange, and fluorescence anisotropy assay** a) elution profile of IMAC and peak fractions loaded to a 12% gel b) elution profile of gel filtration and samples loaded to a 12% gel c) elution profile of gel filtration after nucleotide exchange reaction and samples loaded to a 12% gel d) – f) HPLC of d) GDP e) GMPPNP f) purified MBP-Cdc42 g) MBP-Cdc42.GMPPNP h) to j) mass spectrometry data for MBP-Cdc42 h) deconvoluted spectrum from charge states in m/z range: 813-923 from LC-MS, denaturing condition; mass for Cdc42 is measured to be 60359.37 Da (calculated 60358.9 Da) i) deconvoluted spectrum from native MS for purified MBP-Cdc42, mass difference between empty (denatured) MBP-Cdc42 and native, purified Cdc42 of 467.70 Da fits mass of GDP and bound $Mg^{2+}$ (calculated 465.32 Da) j) deconvoluted spectrum from native MS for GMPPNP exchanged MBP-Cdc42, mass difference between empty (denatured) MBP-Cdc42 and native MBP-Cdc42.GMPPNP of 544.20 Da fits mass of GMPPNP and bound $Mg^{2+}$ (calculated 544.32 Da) k) fluorescence anisotropy assay of purified MBP-Cdc42 and the GMPPNP loaded MBP-Cdc42 with the FITC-labeled CRIB peptide of CeMRCK1

had its elution maximum at 3.68 ml (Figure 7 g), GMPPNP eluting at 3.57 ml (Figure 7 e), indicating that nucleotide exchange was successful. As for Cdc42, a sample was prepared for mass spectrometry (Figure h to j) and the successful nucleotide reaction could be verified. The GMPPNP-loaded MBP-Cdc42 was titrated in a fluorescence anisotropy assay in increasing concentrations up to 60 µM to the FITC-labeled CRIB-peptide, but no binding could be detected (Figure 7 h). As a negative control, the purified GDP-loaded MBP-Cdc42 was titrated to the CRIB-peptide.

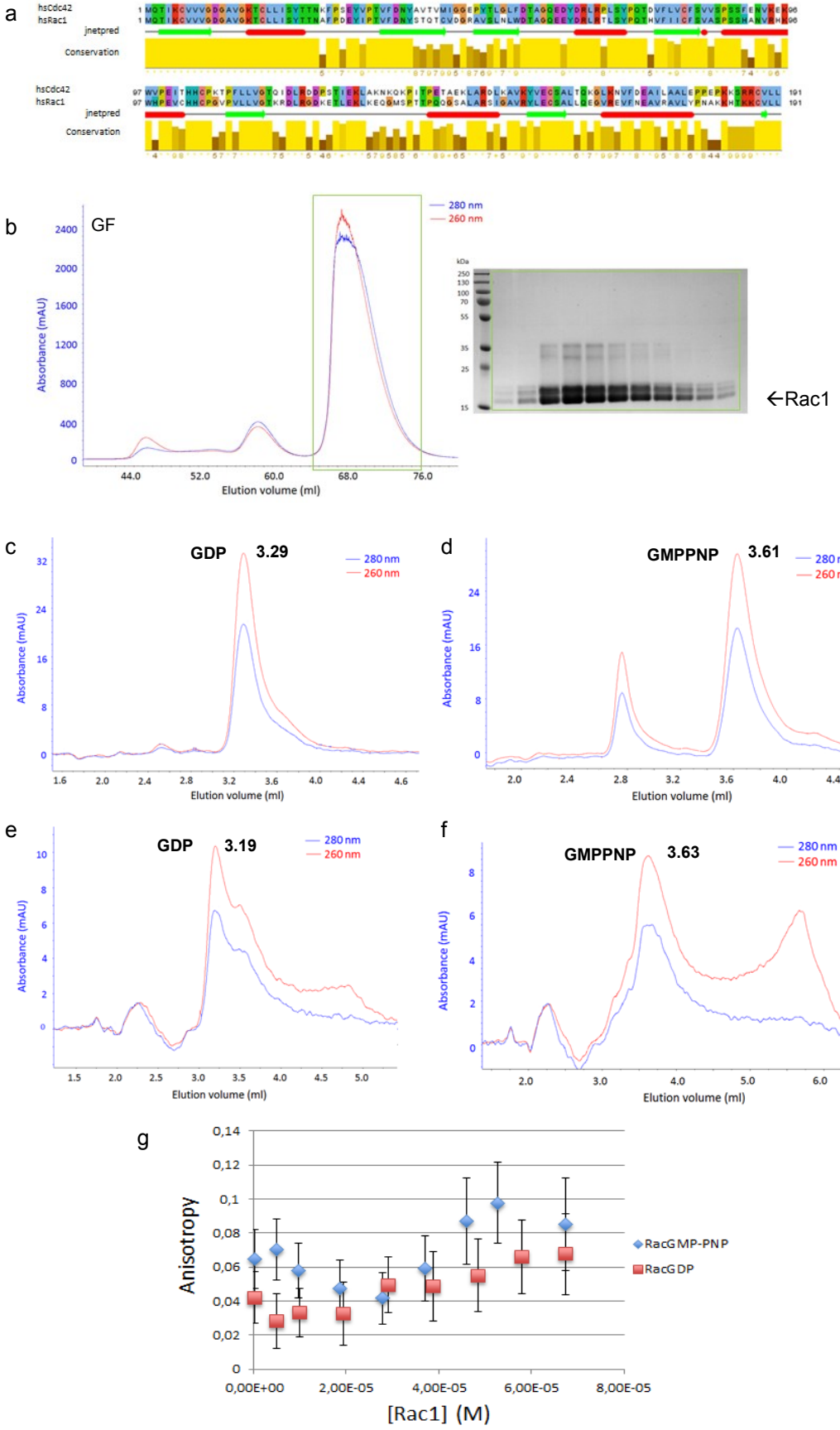


**Figure 8 Rac1 purification, nucleotide exchange, and fluorescence anisotropy assay** a) alignment of hsCdc42 and hsRac1 b) gel filtration of hsRac1 c) to f) HPLC of c) GDP d) GMPPNP e) purified Rac1 f) Rac1.GMP-PNP g) fluorescence anisotropy assay of Rac1 and the CRIB peptide of CeMRCK1

## 3.6 Interaction of Rac1 with MRCK

HsRac1 terminates in the same CAAX-motif as Cdc42. Addition of a geranylgeranyl isoprenoid lipid to the cysteine is important for membrane attachment. To be able to purify the soluble protein, amino acids 2-178 of Rac1 were cloned as a GST-fusion protein, expressed in *E. coli*, and purified according to the protocol for Cdc42 (Figure 8 b). To ensure that the GTPase is in its active state, GDP was exchanged for the non-hydrolysable GMPPNP in the presence of Dbs. The exchange reaction was successfully verified via IP-RP HPLC, with a peak maximum for GDP at 3.29 ml (Figure 8 c) and for GMPPNP at 3.63 ml elution volume (Figure 8 d) and peak maxima for the purified and the GMPPNP loaded Rac1 at 3.19 ml and 3.61 ml, respectively (Figure 8 e and f). Fluorescence anisotropy did not reveal any binding of either Rac1-GDP or Rac1-GMPPNP to the FITC-labeled CRIB-peptide (Figure 8 g).

# 4 DISSCUSION

Here we investigated the structure and function of the C-terminal regulatory domains of myotonic dystrophy kinase related Cdc42-binding kinase. A crystal structure is only available of the kinase domain (Heikkila et al. 2011) and the regulatory C-terminal domains have been hardly addressed in publications available to date. It has been shown that the C1 domain of MRCK is binding to phorbol esters (Choi et al. 2008) but no other study to date has explicitly addressed the interaction of the C1 domain with diacylglycerol. The question remains, whether the C1 domain of MRCK alone mediates the interaction with the membrane via binding to DAG, or whether there is coincident detection of multiple membrane-embedded ligands by the C1, PH, and CNH domains. No studies to date have addressed the PH or CNH domains of MRCK. The PH domain is assumed to trigger interaction with the membrane, since this is the case for other proteins harboring a PH domain. However, the interaction of MRCK's PH domain with membranes has not been investigated and the CNH domain is the least well characterized in terms of structure and function.

Identified in the citron kinase CRIK, the role of the CNH domain has never been addressed in the context of MRCK. The CNH domains in TNIK (TRAF2 and NCK-interacting protein kinase) and Misshapen-like kinase 1 (MINK) have been shown to bind to the small GTPase Rap2 (Hussain et al. 2010) and to interact with the kinase domain leading to autoinhibition of the kinase (Mikryukov & Moss 2012). The CNH domain of the lysosomal tethering/docking factor hVam6p has been suggested to interact with lipids on lysosomal membranes important for lysosome fusion (Caplan et al. 2001). The role of the CNH domain in MRCK is completely unknown. The basic folds for the C1 and the PH domains are known from homologous structures in the protein data bank, but there is no homologous structure for the CNH domain available. We do not know the explicit structures of the individual C-terminal domains of MRCK, how they are arranged with respect to each other in the three dimensional structure of the holoenzyme, what their putative lipid ligands are, and how they are involved in the interaction of MRCK with cellular membranes. We suggest that the C1, PH, and CNH domains act in concert to trigger membrane localization of MRCK. To understand the function of these domains, and especially of the CNH domain, we aimed to solve the structure of the C-terminal region of MRCK. We hope that this will reveal how the domains are arranged and how they interact

with each other. Moreover, we seek to understand MRCK's interaction with the membrane and its localization in the cell.

The fourth regulatory domain of MRCK at its very C-terminal end is the Cdc42-binding CRIB domain. Interaction of Cdc42 with MRCK has been investigated by co-immunoprecipitation and western blotting but the binding has never been investigated or quantitated in vitro. Therefore, the two main goals of this work were to determine the crystal structure of the C-terminal regulatory region and to quantify the binding of Cdc42 to MRCK in solution. The structure of the regulatory domains, together with an understanding of the interaction between MRCK and Cdc42, is expected to help rationalize the targeting of MRCK to membranes in the cell, where it phosphorylates its substrates.

## 4.1 The carboxy-terminal region of MRCK and its interaction with the membrane

MRCK is conserved from sea squirts over mosquitos and frogs to humans. Mammals encode three isoforms of MRCK: MRCKα, MRCKβ, and MRCKγ. They all have the same domain organization with the only difference being the length of the linker regions. Figure 1 a shows the domain organization of the human and the mouse MRCKα as well as the *C. elegans* and the *D. melanogaster* Genghis Khan (GEK) isoforms. The *C. elegans* MRCK1 is slightly shorter than the other homologues, with shorter unstructured regions in the protein. The coiled coil region of MRCK1 is shorter than the coiled coil region in the human homologue but most of the difference in length comes from the shorter C-terminus, which is predicted to be unstructured. The lengths of the single domains are highly conserved among different organisms (Figure 1 b). This makes the *C. elegans* MRCK1 a good candidate for biochemical and structural analysis. Furthermore, attempts to express and purify the C-terminal domains of the human MRCKα protein were unsuccessful. Purification of the CNH domain of CeMRCK1 alone resulted in soluble aggregates. We hypothesized that the regulatory domains may not be separable on the basis of short and highly conserved linkers between the C1, PH, and CNH domains. The start of the construct was therefore designed to include the C1, PH, and CNH domains according to secondary structure predictions and alignment to ancestral orthologues. The construct begins at amino acid 955, prior to the start of the C1 domain and ends at amino acid 1592, the

end of the protein. As such, the construct encompasses the C1, PH, and CNH domains of MRCK. We included the entire C-terminal region, which is predicted to be unstructured, but which also contains the CRIB motif in order to investigate the binding of Cdc42.

MRCK has been shown to bind to membranes in vivo (Gagliardi et al. 2014; Leung et al. 1998; Sung et al. 2008; Unbekandt & Olson 2014) and in 2008 the interaction of the C1 domain of MRCKα with phorbol esters was investigated in vitro (Sung et al. 2008), determining the dissociation constant of the C1 domain for phorbol esters to be in the nanomolar range (Sung et al. 2008; I Tan et al. 2001). Phorbol esters are used as diacylglycerol mimics because they are not turned over by the cell like DAG, and therefore induce a long lasting activation of the kinase compared to the transient activation mediated by DAG. Moreover, phorbol esters are soluble and therefore easier to handle experimentally than DAG itself. One problem with this is that binding of phorbol esters cannot be compared to binding of DAG and therefore do not reflect the native situation in the cell, since these two molecules have different structures. Although they bind to the same pocket they do this in a completely different way. It has been shown that the binding affinities of DAG and phorbol esters for PKC differ and that binding of these proteins have different effects on the kinase (Slater et al. 1994). Therefore, the results of this study are somewhat meaningless, since phorbol ester binding to the C1 domain cannot be compared to DAG binding in the physiological setting.

To evaluate the binding of MRCK to membranes in the absence of known ligands for the PH and CNH domains, we used Folch Fraction 1, which consists of a 1:5:4 ratio of phosphoinositols, phosphatidylserine, and cerebrosides, in order to mimic cell membranes. Since the true ligands for each of the C-terminal domains are unknown, we needed to cover as broad a spectrum of lipids as possible for our experiment, which is why we chose to use a source of lipids extracted from source lipids. We could detect only approximately 45% binding, indicating that the affinity of the isolated regulatory domains was low or that the liposomes are a poor mimic for the specific membranes to which MRCK localizes in vivo. One difficulty here is that specific lipid ligands of MRCK's C-terminal domains are completely unknown and the composition of the lipids used in our binding assay was one first trial for investigating on this issue. Another reason for choosing brain extracts from bovine brain type I is

that MRCK has been shown to be highest expressed in the brain (Leung et al. 1998). Nevertheless, MRCK is also expressed in other tissues (Unbekandt & Olson 2014) and the lipid specificity of the C-terminal domains of MRCK needs further investigation. For the PH domain it is known from a study investigating the lipid-binding characteristics of 91 PH domains from different organisms and different proteins that binding to membranes requires phosphoinositides but binding affinity and binding specificity are dependent on the presence of auxiliary signaling lipids (Vonkova et al. 2016). The membrane binding properties of the PH domains were measured with the help of a liposome-microarray-based assay (LiMA) developed by Saliba et al. (Saliba et al. 2014; Saliba et al. 2016). LiMA integrates liposomes, microfluidics, and fluorescence microscopy to measure membrane binding of proteins in a quantitative and high-throughput manner and it can be scaled up to the lipidome scale (Saliba et al. 2014; Saliba et al. 2016). With this assay it would be possible to systematically test binding of the C-terminal domain of MRCK to different liposome compositions and to investigate the specific lipid ligands of MRCK. If this assay would reveal no high binding affinity for MRCK and membranes, binding of MRCK to membranes in the presence of lipitated, activated Cdc42 would need to be investigated in a next step. It has been shown that interaction of MRCK with Cdc42 has no effect on the kinase activity (Leung et al. 1998) but it was suggested to trigger membrane localization of MRCK (Unbekandt & Olson 2014). Since MRCK interacts with Cdc42, localized to the membrane via its geranyl-geranyl lipid anchor, interaction of MRCK with cellular membranes may not need to be of high affinity in the presence of Cdc42 at the membrane.

## 4.2 Crystallization of MRCK regulatory domains

Our first attempts to crystallize the CeMRCK1 955-1592 construct failed. This might be due to the predicted unstructured region at the very C-terminus that includes the CRIB domain (Figure 1 a and b). The CRIB domain is suggested to be unstructured in the unbound state (Stevens et al. 1999) and since unstructured regions can impair protein crystallization, we sought to identify the unstructured region of CeMRCK1 by limited proteolysis. The protein was incubated with two different proteases, trypsin and chymotrypsin. Both are serine proteases that hydrolyze specific peptide bonds at accessible and therefore unstructured regions of the protein. Limited proteolysis

yielded stable, truncated constructs that could be crystallized in the Morpheus crystallization screen. We determined the truncation of the construct by mass spectrometry, which identified a peptide with a mass of 62982.3 Da, and we identified this truncated protein as comprising amino acids 955-1517. This construct, with an expected mass of 62971.3 Da, best fits the results of intact mass determination, and it would be compatible with trypsin cleavage, since residue 1517 is a lysine and trypsin cleaves its substrates exclusively C-terminal of lysine or arginine residues. The accuracy of mass determination is dependent on the size of the protein to be measured. In this case, the mass of our protein was at the upper limit for the instrument used. Since the raw data was quite noisy, Gaussian smoothing was applied and the mass was determined as the centroid of the peak. This can introduce significant error and may explain the mass discrepancy of 11 Da between the mass spectrometry result and the calculated mass for the 955-1517 construct. The truncation of the protein at residue 1517 corresponds well with secondary structure predictions that indicate that residues 1517-1592 are likely disordered.

All crystallization conditions that yielded protein crystals of the trypsin treated CeMRCK1 construct contained the same precipitant but at different pH values and different additives. Therefore, it seemed most plausible for optimization to screen for precipitant concentration in the first place and to finescreen these crystals for additives such as glycerol and DTT, which might be expected to decrease nucleation. Control of nucleation can also be achieved via microseeding of crystals or streak seeding with a horse hair, which was successful but crystals were hard to reproduce. Finally, different optimization methods were combined for best results.

The final crystals diffracted quite well and revealed space group P1 with six molecules in the asymmetric unit. Space group P1 describes a triclinic unit cell, a primitive lattice that is described by the absence of any internal symmetry. The lattice is therefore composed of repeating translations of the unit cell. In such crystals, each vector is of different length and no vector is at right angles to another. Lattice translations alone reproduced the arrangement of the molecules in the crystal. We obtained a native dataset to 2.3 Å, but attempts to solve the structure by molecular replacement with homologous structures of the C1 and PH domains were unsuccessful. In the absence of phase information with which to solve the structure, selenomethionine-substituted protein was expressed in insect cells and purified. The

incorporation of selenomethionine into the protein could enable us to solve the crystal structure of the desired protein using multi-wavelength anomalous diffraction (MAD). Unfortunately, expression of the selenomethionine-substituted protein led to a much lower protein yield. To circumvent the proteolysis step during purification, and thereby improve yields of the selenomethionine-substituted protein, we decided to prepare recombinant baculovirus for expression of CeMRCK1 955-1517, the construct identified by mass spectrometry. This construct contains the C1, PH, and CNH domains, but is missing the Cdc42-binding CRIB domain (Figure 4 a). Purified CeMRCK1 955-1517 crystallized in similar conditions to the trypsin-treated CeMRCK1 955-1592. Expression and purification of selenomethionine-substituted CeMRCK1 955-1517 is currently in progress. This work will be continued by Dr. Linda Trübestein. It is expected that the crystal structure of the C-terminal domain will reveal important insights into the arrangement of the regulatory domains, putative lipid ligands, and how the three domains together mediate localization of MRCK to cellular membranes. In particular, the structure and function of the CNH domain is of interest given the lack of a homologous structure in the protein data bank.

## 4.3 Interaction of MRCK with the small GTPase Cdc42

The second part of my work was focusing on the interaction between MRCK and Cdc42. MRCK is known to be a downstream effector of the small GTPase Cdc42 and binding of Cdc42 to the CRIB domain was the basis for the identification of MRCKα (Leung et al. 1998). Cdc42 is highly conserved between different species, as shown in figure 5 a. We expressed and purified the human Cdc42 homologue for our experiments. The *C. elegans* homologue exhibits seven amino acid substitutions but all of them are located on surfaces remote from the effector binding surfaces so we were confident that HsCdc42 would behave in an identical manner to CeCdc42 (Figure 5 a). Cdc42 is active in its GTP loaded form but since GTP is hydrolyzed to GDP very easily, GDP had to be exchanged for the non-hydrolyzable GMPPNP or GTPγS. Cdc42 was stoichiometrically loaded with GMPPNP or GTPγS using the guanosine nucleotide exchange factor Dbs and validated by IP-RP HPLC and mass spectrometry. Dissociation constants for other CRIB domain containing proteins and Cdc42 have been measured in the nanomolar range (Garrard et al. 2003; Morreale et al. 2000; Zhang et al. 1997; Schwarz et al. 2012; Mott et al. 1999), and the

interaction between MRCK and Cdc42 has been suggested to be of high affinity (Unbekandt & Olson 2014; Leung et al. 1998; Tan et al. 2003; Huo et al. 2011) though the actual affinity has not been determined. Given reported nanomolar binding constants for other Cdc42 effectors, we first tried to establish complex formation by gel filtration. Surprisingly, no complex formation could be detected: MRCK and Cdc42 eluted separately from the column. The absence of complex formation could be explained by a lower affinity than expected. Moreover, it is also possible that the CRIB domain is not accessible for Cdc42 binding and that other factors are needed to facilitate binding of Cdc42 to MRCK. Therefore, we tested binding of Cdc42 to the CRIB domain alone. The extended CRIB peptide was determined according to secondary structure prediction and conservation among ancestral orthologues (Figure 6 d). However, a pull-down assay again failed to detect binding of Cdc42 to the CRIB peptide. From this we concluded that inaccessibility of the CRIB domain is not the reason for the absence of binding. Having established that the binding must be of weaker affinity than can be detected by size exclusion chromatography or pull-down assay, we decided to perform a fluorescence anisotropy assay to determine the binding affinity of Cdc42 for the CRIB domain. Using GTPγS-loaded Cdc42 and FITC-labelled CRIB peptide we could detect a concentration-dependent increase in anisotropy consistent with binding. Using Cdc42.GDP, we could not detect this increase. Although the binding curve does not reach saturation, we could estimate the binding constant to be approximately 20 µM. However the small increase in anisotropy means that the intrinsic error in the measurement is high and in the absence of saturation the estimate of affinity is subject to errors in the curve fitting.

In fluorescence anisotropy a fluorophore is excited with polarized light resulting in emission of polarized light. However, molecules are tumbling in solution due to the Brownian motion and consequently, the emitted light is differently polarized than the excitation light. The rate of this tumbling and therefore the change in polarization of the emitted light compared to the excitation light is dependent on the size of the complex. Since Cdc42 has a mass of 20 kDa, binding to the 3.4 kDa CRIB peptide does not lead to big changes in rotational diffusion of the fluorophore, which is why we obtain only a small increase in anisotropy. Therefore, to improve the signal in our assay, Cdc42 was fused N-terminally to MBP to generate a protein of 60

kDa instead of Cdc42 alone, which has a mass of 20 kDa. Interestingly, no binding of the MBP fusion protein to the CRIB domain could be detected. It is unlikely that MBP prevents binding, since it could be purified easily and the nucleotide exchange reaction worked as efficiently as for Cdc42 alone. Mass spectrometry verified the successful purification of Cdc42 and MBP fusion protein, and that Cdc42 and MBP-Cdc42 are both stoichiometrically loaded with GMPPNP. At this point, we cannot detect an interaction of measurable affinity between Cdc42 and MRCK, suggesting that the interaction, if real, is intrinsically weak. Further experiments in order to saturate the binding curve are required, possibly also in conjunction with mutations in the peptide that would abrogate binding.

MRCK was originally identified in a screen for effector proteins of Cdc42 by co-immunoprecipitation and western blotting (Leung et al. 1998; Schwarz et al. 2012) but the interaction has not been verified or quantitated in vitro. For binding of Cdc42 to the CRIB domain we obtained an estimated dissociation constant of 20 µM. Detection of protein partners with this low binding affinity would not be expected by co-immunoprecipitation. Another problem of co-IP and western blotting are the antibodies used to detect the protein of interest, since antibodies may exhibit off-target binding. The question arises, whether Cdc42 is actually binding to MRCK. We need to repeat the anisotropy binding assay including a positive control, to ascertain that an interaction similar to the Cdc42-MRCK interaction are detected by the fluorescence anisotropy assay, preferably one that is already known and quantitated in literature (e.g. the binding affinity for Cdc42 and $\alpha PAK_{75-132}$ was determined to be 0.02 µM using the SPA technology (Thompson et al. 1998)).

## 4.4 Interaction of MRCK with Rac1

In addition to Cdc42, Rac1 has been shown to bind to CRIB domains of other proteins as well as to the MRCK-CRIB domain (I Tan et al. 2001; Lee et al. 2014; Burbelo et al. 1995; Tan et al. 2003). Accordingly, we tested the binding of activated Rac1 to the C. elegans MRCK1 CRIB domain via fluorescence anisotropy but we could not detect any binding of Rac1 to the CeMRCK1 CRIB domain. Binding of Cdc42 to MRCK was reported to be of higher affinity than binding of Rac1 (Leung et al. 1998; Tan et al. 2003), but a splice variant of MRCKα transcripts with a tandem CRIB domain showed a strong, but unquantified, interaction with Rac1 (Tan et al.

2003). MRCKα is the only CRIB domain containing protein reported to have this tandem CRIB domain. Moreover, no other studies have explicitly addressed interaction of Rac1 with MRCK. We again were not able to detect an interaction of measurable affinity in vitro which makes interaction of these two proteins unlikely but at this point we cannot eliminate the possibility of an interaction between MRCK and Rac1 in vivo.

In conclusion, we were able to crystallize the C-terminal region of CeMRCK1 without the CRIB domain but we have so far not been able to solve the structure. We have expressed and purified selenomethionine-substituted protein and demonstrated that it can be purified to homogeneity as for native CeMRCK1. We have prepared recombinant baculovirus for expression of a truncated construct comprising residues 955-1517 and we expect to be able to set up crystallization screens for selenomethionine-substituted protein soon. We anticipate being able to solve the structure by MAD at the selenium edge, assuming that we are able to obtain diffracting crystals of the selenomethionine-substituted protein. However, we were unable to identify a high-affinity interaction between MRCK and Cdc42 or Rac1 and further studies will be required to confirm whether in fact there is a productive interaction between these proteins.

# REFERENCES

Burbelo, P.D., Drechsel, D. & Hall, A., 1995. A conserved binding motif defines numerous candidate target proteins for both Cdc42 and Rac GTPases. *Journal of Biological Chemistry*, 270(49), pp.29071–29074.

Caplan, S. et al., 2001. Human Vam6p promotes lysosome clustering and fusion in vivo. *The Journal of cell biology*, 154(1), pp.109–122.

Chandrashekar, R. et al., 2011. A switch I mutant of Cdc42 exhibits decreased conformational freedom. *Biochemistry*, 50(28), pp.6196–6207.

Chircop, M., 2014. Rho GTPases as regulators of mitosis and cytokinesis in mammalian cells. *LANDES Biosciences*, (April), pp.37–41.

Choi, S.H. et al., 2008. Characterization of the interaction of phorbol esters with the C1 domain of MRCK (myotonic dystrophy kinase-related Cdc42 binding kinase) alpha/beta. *The Journal of biological chemistry*, 283(16), pp.10543–9.

Conti, M.A. & Adelstein, R.S., 2008. Nonmuscle myosin II moves in new directions. *Journal of Cell Science*, 121(Pt 1), pp.11–18.

Gagliardi, P.A. et al., 2014. PDK1-mediated activation of MRCKα regulates directional cell migration and lamellipodia retraction. *Journal of Cell Biology*, 206(3), pp.415–434.

Gally, C. et al., 2009. Myosin II regulation during C. elegans embryonic elongation: LET-502/ROCK, MRCK-1 and PAK-1, three kinases with different roles. *Development*, 136(18), pp.3109–3119.

Garrard, S.M. et al., 2003. Structure of Cdc42 in a complex with the GTPase-binding domain of the cell polarity protein, Par6. *EMBO Journal*, 22(5), pp.1125–1133.

Gomes, E.R., Jani, S. & Gundersen, G.G., 2005. Nuclear Movement Regulated by Cdc42, MRCK, Myosin, and Actin Flow Establishes MTOC Polarization in Migrating Cells. *Cell*, 121(3), pp.451–463.

Heikkila, T. et al., 2011. Co-crystal structures of inhibitors with MRCKb, a key regulator of tumor cell invasion. *PLoS ONE*, 6(9), pp.20–22.

Huo, L. et al., 2011. Cdc42-dependent formation of the ZO-1/MRCKβ complex at the leading edge controls cell migration. *The EMBO journal*, 30(4), pp.665–678.

Hussain, N.K. et al., 2010. MINK and TNIK differentially act on Rap2-mediated signal transduction to regulate neuronal structure and AMPA receptor function. *The Journal of*

*neuroscience : the official journal of the Society for Neuroscience*, 30(44), pp.14786–14794.

Johnson, D.I., 1999. Cdc42: An essential Rho-type GTPase controlling eukaryotic cell polarity. *Microbiology and molecular biology reviews : MMBR*, 63(1), pp.54–105.

Lee, I.C.J., Leung, T. & Tan, I., 2014. Adaptor protein LRAP25 mediates myotonic dystrophy kinase-related Cdc42-binding kinase (MRCK) regulation of LIMK1 protein in lamellipodial F-actin dynamics. *Journal of Biological Chemistry*, 289(39), pp.26989–27003.

Lemmon, M.A. & Ferguson, K.M., 2000. Signal-dependent membrane targeting by pleckstrin homology (PH) domains. *The Biochemical journal*, 350 Pt 1, pp.1–18.

Leung, T. et al., 1998. Myotonic dystrophy kinase-related Cdc42-binding kinase acts as a Cdc42 effector in promoting cytoskeletal reorganization. *Mol Cell Biol*, 18(1), pp.130–140.

Lowe, H.I.C. et al., 2012. Cycloartane-3,24,25-triol inhibits MRCKα kinase and demonstrates promising anti prostate cancer activity in vitro. *Cancer cell international*, 12(1), p.46.

Luo, L. et al., 1997. Genghis Khan (Gek) as a putative effector for Drosophila Cdc42 and regulator of actin polymerization. *Proceedings of the National Academy of Sciences of the United States of America*, 94(24), pp.12963–8.

Melendez, J., Grogg, M. & Zheng, Y., 2011. Signaling role of Cdc42 in regulating mammalian physiology. *Journal of Biological Chemistry*, 286(4), pp.2375–2381.

Mikryukov, A. & Moss, T., 2012. Agonistic and Antagonistic Roles for TNIK and MINK in Non-Canonical and Canonical Wnt Signalling M. Klymkowsky, ed. *PLoS ONE*, 7(9), p.e43330.

Morreale, a et al., 2000. Structure of Cdc42 bound to the GTPase binding domain of PAK. *Nature structural biology*, 7(5), pp.384–388.

Mott, H.R. et al., 1999. Structure of the small G protein Cdc42 bound to the GTPase-binding domain of ACK. *Nature*, 399(6734), pp.384–388.

Nakamura, N. et al., 2000. Phosphorylation of ERM proteins at filopodia induced by Cdc42. , 1, pp.571–582.

Ng, Y. et al., 2004. Expression of the human myotonic dystrophy kinase-related Cdc42-binding kinase g is regulated by promoter DNA methylation and Sp1 binding. *Journal of Biological Chemistry*, 279(33), pp.34156–34164.

Ono, Y. et al., 1989. Phorbol ester binding to protein kinase C requires a cysteine-rich zinc-finger-like sequence. *Proceedings of the National Academy of Sciences of the United States of America*, 86(13), pp.4868–71.

Pollard, T.D. & Cooper, J.A., 2009. Actin, a Central Player in Cell Shape and Movement. *Science (New York, N.Y.)*, 326(5957), pp.1208–1212.

Rudolph, M.G. et al., 1998. The Cdc42/Rac interactive binding region motif of the Wiskott Aldrich syndrome protein (WASP) in necessary but not sufficient for tight binding to Cdc42 and structure formation. *Journal of Biological Chemistry*, 273(29), pp.18067–18076.

Saliba, A.-E. et al., 2016. A protocol for the systematic and quantitative measurement of protein-lipid interactions using the liposome-microarray-based assay. *Nat. Protocols*, 11(6), pp.1021–1038.

Saliba, A.-E. et al., 2014. A quantitative liposome microarray to systematically characterize protein-lipid interactions. *Nat Meth*, 11(1), pp.47–50.

Schwarz, J. et al., 2012. Serine-71 phosphorylation of Rac1 modulates downstream signaling. *PloS one*, 7(9), p.e44358.

Slater, S.J. et al., 1994. Evidence for discrete diacylglycerol and phorbol ester activator sites on protein kinase C. Differences in effects of 1-alkanol inhibition, activation by phosphatidylethanolamine and calcium chelation. *Journal of Biological Chemistry* , 269 (25 ), pp.17160–17165.

Stengel, K. & Zheng, Y., 2011. Cdc42 in oncogenic transformation, invasion, and tumorigenesis. *Cellular signalling*, 23(9), pp.1415–1423.

Stevens, W.K. et al., 1999. Conformation of a Cdc42/Rac interactive binding peptide in complex with Cdc42 and analysis of the binding interface. *Biochemistry*, 38(19), pp.5968–5975.

Sung, H.C. et al., 2008. Characterization of the interaction of phorbol esters with the C1 domain of MRCK (myotonic dystrophy kinase-related Cdc42 binding kinase) α/β *Journal of Biological Chemistry*, 283(16), pp.10543–10549.

Tan, I. et al., 2008. A Tripartite Complex Containing MRCK Modulates Lamellar Actomyosin Retrograde Flow. *Cell*, 135(1), pp.123–136.

Tan, I. et al., 2003. Genomic organization of human myotonic dystrophy kinase-related

Cdc42-binding kinase alpha reveals multiple alternative splicing and functional diversity. *Gene*, 304, pp.107–15.

Tan, I. et al., 2001. Intermolecular and intramolecular interactions regulate catalytic activity of myotonic dystrophy kinase-related Cdc42-binding kinase alpha. *Molecular and cellular biology*, 21(8), pp.2767–78..

Thompson, G. et al., 1998. Delineation of the Cdc42 / Rac-Binding Domain of p21-Activated Kinase. *Biochemistry*, 37(21), pp.7885–7891.

Unbekandt, M. et al., 2014. A novel small-molecule MRCK inhibitor blocks cancer cell invasion. *Cell communication and signaling : CCS*, 12(1), p.54.

Unbekandt, M. & Olson, M.F., 2014. The actin-myosin regulatory MRCK kinases: Regulation, biological functions and associations with human cancer. *Journal of Molecular Medicine*, 92(3), pp.217–225.

Vicente-Manzanares, M. et al., 2009. Non-muscle myosin II takes centre stage in cell adhesion and migration. *Nature Reviews Molecular Cell Biology*, 10(11), pp.778–790.

Vonkova, I. et al., 2016. Lipid Cooperativity as a General Membrane-Recruitment Principle for PH Domains. *Cell Reports*, 12(9), pp.1519–1530.

Wilkinson, S., Paterson, H.F. & Marshall, C.J., 2005. Cdc42-MRCK and Rho-ROCK signalling cooperate in myosin phosphorylation and cell invasion. *Nature cell biology*, 7(3), pp.255–261.

Wu-Zhang, A.X. & Newton, A.C., 2013. Protein Kinase C Pharmacology: Refining the Toolbox. *The Biochemical journal*, 452(2), pp.195–209.

Zhang, B., Wang, Z. & Zheng, Y., 1997. Characterization of the Interactions between the Small GTPase Cdc42 and Its GTPase-activating Proteins and Putative Effectors. *The Journal of Biological Chemistry*, 272(35), pp.21999–22007.

# APPENDIX

## List of Figures



## List of Tables

## Abstract

MRCK (Myotonic dystrophy kinase-related Cdc42-binding kinase) is a member of the AGC superfamily of Rho-activated serine/threonine kinases and it plays a role in the regulation of cytoskeletal reorganization and cell migration. In addition to the amino-terminal kinase domain, which is important for phosphorylation of its substrates (e.g. myosin light chain), the carboxy-terminus of MRCK is important for the interaction with other proteins and the membrane. This C-terminal region of MRCK contains a C1 domain, a pleckstrin homology (PH) domain, a citron homology (CNH) domain, and the Cdc42/Rac interactive binding (CRIB) domain, which is said to bind to the GTP-activated form of the small GTPase Cdc42 and with a lower affinity to the small GTPase Rac1. To date, there is no information available about the three dimensional arrangement of these C-terminal domains, about its putative lipid ligands, and about their role in membrane targeting of MRCK.

The aim of this master's thesis is to understand the role of the C-terminal domains in membrane localization. This involves solving the crystal structure of the regulatory C-terminal region and the quantification of the interaction of MRCK with Cdc42.

A lipid binding assay revealed 45 % of MRCK C-terminal regions binding to brain lipids. Protein crystals of the C-terminal region excluding the CRIB domain yielded a diffraction data that revealed space group P1 with 6 atoms in the unit cell. We obtained a native dataset to 2.3 Å, but attempts to solve the structure by molecular replacement with homologous structures of the C1 and PH domains were unsuccessful.

To investigate the interaction between MRCK and Cdc42, different experiments were conducted revealing no (or very low) binding between these two proteins. With the help of fluorescence anisotropy an estimated dissociation constant of 20 µM could be measured. An attempt to improve the binding curve with an MBP-Cdc42 fusion protein was unsuccessful. A fluorescence anisotropy assay using Rac1 as binding partner for MRCK showed no binding as well. The crystal structure of the MRCK carboxy-terminal region could not be solved, but X-ray diffractable crystals were grown and we suppose to be able to solve the structure by multi-wavelength anomalous diffraction (MAD) at the selenium edge.

The binding of Cdc42 to MRCK could not be satisfactorily verified, which leads to the question, whether the interaction of these two proteins actually involves direct binding. Further experiments will shed light on this.

## Zusammenfassung

MRCK ist eine Serin/Threonin-Kinase der AGC Superfamilie, die durch Mitglieder der Familie der Rho-GTPasen aktiviert werden. MRCK spielt eine wichtige Rolle in der Umstrukturierung des Cytoskelettes und der Zellbewegung. Zusätzlich zu der amino-terminalen katalytischen Domäne, die für die Phosphorylierung der Substrate wichtig ist (z.B. die leichten Ketten von Myosin), besitzt MRCK mehrere carboxy-terminale Domänen, die für die Wechselwirkung mit anderen Proteinen und der Membran wichtig sind. Diese C-terminale Region beinhaltet eine C1 Domäne, eine Pleckstrin-Homologie (PH) Domäne, eine Citron-Homologie (CNH) Domäne, und die sogenannte CRIB-Domäne, welche die aktivierte, GTP-gebundene Form der kleinen GTPase Cdc42 und mit geringerer Affinität auch Rac1 bindet. Aktuell ist nicht bekannt, wie diese C-terminalen Domänen drei dimensional angeordnet sind, welche möglichen Lipid-Liganden sie haben, und welche Rolle sie in der Membranlokalisierung von MRCK spielen.

Das Ziel dieser Masterarbeit ist es, die Rolle der C-terminalen Domänen in der Membranlokalisierung zu verstehen. Das involviert die Aufklärung der Kristallstruktur der regulatorischen C-terminalen Region, sowie die Quantifizierung der Wechselwirkung zwischen MRCK mit Cdc42.

Ein Lipid-Bindeassay ergab, dass 45 % MRCK (C-terminale Region) an Hirn-Lipide binden. Proteinkristalle der C-terminalen Region ohne der CRIB-Domäne lieferten Beugungsdaten, die die Raumgruppe P1 mit sechs Atomen in der Einheitszelle ergaben. Wir erhielten einen nativen Datensatz bis 2.3 Å, aber Versuche, die Struktur durch „Molecular Replacement“ mit homologen Strukturen der C1 und PH Domänen aufzuklären, waren nicht erfolgreich.

Um die Wechselwirkung zwischen MRCK und Cdc42 zu untersuchen wurden verschiedene Experimente durchgeführt, die keine (oder nur sehr schwache) Bindung zwischen diesen zwei Proteinen ergaben. Mit Hilfe der Fluoreszenzanisotropie konnte eine Dissoziationskonstante für Cdc42 und MRCK von 20 µM gemessen werden. Der Versuch, die Bindungskurve mit einem MBP-Cdc42 Fusionsprotein zu verbessern, ergab jedoch keinerlei Bindung, genauso wie Untersuchungen mit Rac1 als Bindungspartner. Die Kristallstruktur der carboxy-terminalen Domäne konnte nicht aufgeklärt werden, aber Kristalle, die Röntgenstrahlen beugen, konnten gezüchtet werden und wir erwarten, die

Kristallstruktur mit Hilfe des Selenomethionin-substituierten Proteins und der „Multiwavelength anomalous dispersion“ (MAD)-Methode lösen zu können.

Die Bindung zwischen Cdc42 und MRCK konnte nicht zufriedenstellend nachgewiesen werden, was zu der Frage führt, ob die Wechselwirkung zwischen diesen beiden Proteinen tatsächlich das direkte Binden von Cdc42 an die CRIB-Domäne involviert. Weitere Experimente werden darüber Aufschluss geben